C1 p

FACILITY FORM 602

N65-35217 (ACCESSION NUMBER)	(THRU)
61 (PAGES)	1 (CODE)
TMX-54614 (NASA CR OR TMX OR AD NUMBER)	30 (CATEGORY)

REENTRY

by

(NASA TMX-54614)

E. Brian Pritchard [1963] 61p refs

National Aeronautics and Space Administration

Langley Research Center, Langley Station, Va.

Hampton, Virginia

Presented At

The Inter-American Institute for Space Science Education

1963 Summer Conference for Science Teachers

☐ Conf

[redacted]

GPO PRICE $ ______

CFSTI PRICE(S) $ ______

Hard copy (HC) 3.00

Microfiche (MF) .75

ff 653 July 65

Reentry

by

E. Brian Pritchard

Introduction

Any manned space mission is composed of several distinct phases: the launch phase, the accomplishment of mission objectives phase, and the reentry phase. We are concerned here with the final or reentry phase of the space mission. It is during this period that the uncorrectable errors accrued during the space mission must be overcome in order to safely land the reentry vehicle at the desired landing site.

During the launch phase a vast amount of kinetic energy must be imparted to the space vehicle in order that it may escape from the earth and accomplish its mission. In returning to earth after completion of the mission, this same amount of kinetic energy must be dissipated in some manner. There are two ways in which this may be accomplished: rocket braking or atmospheric braking. The use of rocket braking allows the space vehicle to reenter the atmosphere at low speeds, thus essentially eliminating the reentry problem. However, due to the huge weight penalities associated with rocket braking this method of energy dissipation is not practical. Atmospheric braking, wherein the vehicle kinetic energy is dissipated by aerodynamic drag as the vehicle travels through the atmosphere, is much more favorable as may be seen in Figure 1.

In this figure the vehicle uses aerodynamic braking below satellite velocity and the weight ratio presented is the ratio of the vehicle weight at any velocity to the vehicle weight for reentry at satellite velocity. As shown, atmospheric braking, where the increasing weight is due to the additional thermal protection required as the reentry velocity increases, is much more favorable than rocket braking.

It should be noted that the aerodynamic or ablation curve shown here is quite conservative since it is assumed that the vehicle has a lift-drag ratio capability of one and that the stagnation point heating applies over the entire vehicle. Thus, the ablation weights shown are much higher than is actually the case. But, even under the worst possible conditions aerodynamic, ablation cooled braking is far superior to rocket braking.

Therefore, since minimum weight must be the prime consideration, atmospheric braking is required to dissipate the kinetic energy attained during a space mission. The reentry of a vehicle into the earth's atmosphere at high velocities thus becomes a major problem. In studying reentry one immediately can forsee several broad problem areas associated with the safe return of a manned vehicle from space to a desired landing site on the earth's surface. These are:

A. Deceleration Loads

B. Reentry Corridor Width

C. Aerodynamic Heating

    1. Convective

    2. Radiative

D. Range Control

1. Longitudinal

2. Lateral

For a given space mission, the above problem areas define the reentry vehicle design. Thus we have the Mercury, Gemini, Apollo, and Dynasoar reentry vehicles (each designed for a different mission).

It is the purpose here to define the reentry equations of motion and investigate each of the reentry problem areas in some detail. Means of alleviating these problems by proper vehicle design will be demonstrated. A range of initial reentry velocity from satellite velocity to a reentry velocity of 100,000 ft/sec is chosen to illustrate the increase in reentry vehicle refinement required by increasing reentry velocity.

Equations of Motion

Consider a vehicle at some point along its reentry path with the aerodynamic and gravitational forces acting as shown.

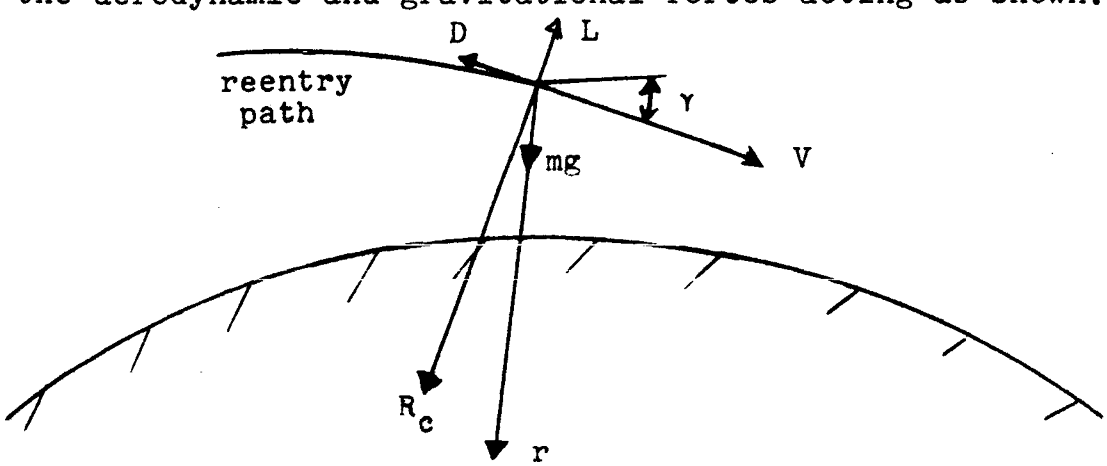

Writing the equation of motion along the flight path one obtains:

$$\frac{mdV}{dt} = -D - mg \sin \gamma \tag{1}$$

or

$$\frac{1}{g}\frac{dV}{dt} = \frac{-\rho V^2}{2(\frac{W}{C_D A})} - \sin \gamma \tag{2}$$

The equation of motion perpendicular to the flight path is:

$$\frac{-mV^2}{R_c} = -mV^2 \left(\frac{\cos \gamma}{r} - \frac{1}{V}\frac{d\gamma}{dt}\right) = L - mg \cos \gamma \tag{3}$$

or

$$\frac{d\gamma}{dt} = \frac{g}{V} \left\{\frac{\rho V^2}{2(\frac{W}{C_D A})} \frac{L}{D} - \cos \gamma (1 - \frac{V^2}{rg})\right\} \tag{4}$$

Additional equations of interest are:

$$\frac{dh}{dt} = V \sin \gamma \tag{5}$$

and

$$\frac{d(\frac{R}{r_e})}{dt} = \frac{V}{r} \cos \gamma \tag{6}$$

Equations 2, 4, 5, and 6 must then be solved simultaneously to achieve a solution. In general a high speed digital computer is required to solve these equations of motion. Analytical solutions are available however for certain maneuvers of interest which will be discussed in more detail subsequently.

VARIATION OF ENTRY VELOCITY WITH ENTRY ANGLE

In analyzing the reentry phase of a space mission it is generally assumed that the initial reentry velocity is invariant with the initial reentry angle. To determine the applicability of this assumption let us consider the return of a vehicle from a circular orbit about the earth. For the condition of retro-fire along the orbital track it may be shown that the initial reentry velocity and angle are related by the expression:

$$V_i^2 = 2\, r_o^2 g_o \left\{ \frac{1}{r_i} - \frac{r_i \cos^2 \gamma_i - r_2}{r_i^2 \cos^2 \gamma_i - r_2^2} \right\} \qquad (7)$$

where i = initial entry conditions

o = earth surface conditions

2 = point of retrofire conditions

Equation 7 is plotted in Figure 2 for a range of initial entry angles from 0 degrees to 12 degrees which should encompass the reentry corridor boundaries for vehicles of interest. As shown, initial reentry velocity is essentially invariant for return from orbital altitudes greater than about 2,000 miles. Therefore, we may say that, if the apogee altitude of the space mission is greater than 2,000 miles, the initial reentry velocity is independent of the initial reentry angle.

ATMOSPHERIC MANEUVERS

A vehicle reentering the earth's atmosphere following a deep space mission must be capable of aerodynamic maneuvering since deviations from the desired entry conditions will occur due to guidance and control system inaccuracies encountered during the mission.

The trajectories traversed during reentry by an uncontrollable and a controllable vehicle are illustrated in Figure 3. As shown, a vehicle incapable of aerodynamic maneuvers will, in general, skip outside of the atmosphere. Maneuverability is required in order to reduce the maximum deceleration loads to tolerable levels and control the range traversed so as to land at some preselected site.

The "g" control maneuver requires that the reentry vehicle have the capability to vary the angle of attack from the angle for maximum lift to that for zero lift. To achieve range control, the vehicle must have the capability of either angle of attack variation or roll angle variation such that the vehicle lift-drag ratio may be varied or modulated during the reentry period. Of the two maneuvers the range control maneuver is of the greater importance since the "g" control maneuver (discussed subsequently) would probably be used only in an emergency condition. The primary maneuvers considered for the range control problem are presented in Figure 4.

In general, the range control maneuver is initiated after the region of peak deceleration load and aerodynamic heating rate has been passed. Approximately minimum ranges are attainable by the constant heating rate and constant "g" maneuvers and maximum ranges by the constant altitude, equilibrium glide, and constant L/D-skip maneuvers. As shown, the constant $\dot{q}$ trajectory may not be maintained for a long period of time since the deceleration load is continually increasing during this maneuver and will exceed acceptable limits. It is therefore not a practical maneuver, and is not considered further.

The constant "g" maneuver is one in which the deceleration load is maintained at a constant level by roll control. By maintaining the deceleration load at a comparatively high level, the vehicle's kinetic energy is rapidly dissipated and minimal ranges are obtained. An analytical solution is available for this maneuver with the assumption of an exponential density-altitude relationship given by:

$$\frac{\rho}{\rho_o} = e^{-\beta h} \tag{8}$$

where ρ_o = sea level density

and β = scale height, $\frac{1}{23,500}$ ft^{-1}.

The reentry equations of motion of interest are:

$$\frac{1}{g}\frac{dV}{dt} = -\frac{G}{\sqrt{1 + (L/D)^2}} - \sin\gamma, \tag{9}$$

where G = constant deceleration load

$$\frac{d\left(\frac{R}{r_e}\right)}{dt} = \frac{V}{r}\cos\gamma \tag{10}$$

and

$$\frac{dh}{dt} = -V\sin\gamma \tag{11}$$

Solution of equations 9, 10, and 11 with the aid of equation 8 yields the following result for the longitudinal range traversed during the maneuver.

$$\frac{R}{r_e} = \frac{\sqrt{1 + (L/D)^2}}{G} \left\{ \frac{\bar{V}_1{}^2 - \bar{V}_2{}^2}{2} - \frac{(h_1 - h_2)}{r_e} \right\} \quad (12)$$

The term $\frac{(h_1 - h_2)}{r_e}$ may be neglected in equation (12) as it is quite small in comparison to the velocity terms. Also, the maneuver end velocity, V_2, may be shown to be given by

$$\bar{V}_2{}^2 = \frac{2}{\beta r_e} \frac{(1 + G)}{\sqrt{1 + (L/D)^2}} \quad (13)$$

The constant altitude maneuver is initiated at the bottom of the pullout by a vehicle initially entering the atmosphere with positive Lift. The vehicle maintains a constant altitude flight path by either pitch or roll modulation.

The sum of the lift and centrifugal force is thus maintained equal to the vehicle weight. Eventually, the velocity decreases to the point where sufficient lift cannot be generated to satisfy this equality. A constant L/D trajectory is then flown to the landing site. For the constant-altitude maneuver the reentry equations of motion reduce to:

$$\frac{L}{W} = 1 - \bar{V}^2 \quad (14)$$

$$\frac{dV}{dt} = - \frac{\rho V^2 g}{2\left(\frac{W}{C_D A}\right)} \quad (15)$$

$$\frac{d\left(\frac{R}{r_e}\right)}{dt} = \frac{V}{r_e} \tag{16}$$

If the maneuver is controlled by roll angle modulation at constant drag coefficient, the longitudinal range may be shown to be given by:

$$\frac{R}{r_e} = -\frac{2\left(\frac{W}{C_D A}\right)}{\rho r_e g} \ln \frac{V_2}{V_1} \tag{17}$$

where V_1 and V_2 are the velocities at the beginning and ending of the maneuver. Control of this maneuver by pitch modulation does not, in general, result in an analytic solution.

The equilibrium glide maneuver is an approximation to the constant L/D maneuver. It is initiated at the point on the constant L/D pullup trajectory defined by the condition:

$$\rho = \frac{(1 - \overline{V}^2)}{\overline{V}^2} \left(\frac{2W}{S}\right) \left(\frac{1}{C_{L_{e.g.}}}\right) \tag{18}$$

where $C_{L_{e.g.}}$ is a constant.

It is then assumed that the flight path angle is negligibly small and that the equality of equation (14) holds. If the maneuver is initiated at velocities greater than local satellite velocity ($\overline{V} > 1$), $C_{L_{e.g.}}$ is negative and the altitude increases (ρ decreases) with decreasing velocity. Note that at $\overline{V} = 1$ an infinite altitude is required. For velocities less than the local satellite value, $C_{L_{e.g.}}$ is positive and the altitude decreases (ρ increases) with decreasing velocity. Obviously some transition maneuver is required in the region of $\bar{V} = 1$ to transfer from the negative equilibrium glide to the positive equilibrium glide maneuver.

It is assumed here that a minimum dynamic pressure of 10 psf is required for aerodynamic maneuvering. Therefore, a maximum range transition maneuver would be one which is carried out at a constant dynamic pressure of 10 psf. This combination of negative equilibrium glide, constant q = 10 psf transition, and positive equilibrium glide should yield approximately maximum range for a wholly atmospheric maneuver.

The equations of motion for this case are given by equations 14 and 15 and may be shown to give the following expression for longitudinal range.

$$\frac{R}{r_e} = \frac{L}{D} \left\{1 + \frac{1}{2} \ln \left[\frac{\bar{V}_1{}^2 - 1}{(\bar{V}_2{}^2 - 1)^2}\right]\right\} \tag{19}$$

where $\bar{V}_2 = \sqrt{1 + \dfrac{10}{\left(\dfrac{W}{C_L A}\right)}}$

The final maximum range maneuver considered here is the true constant L/D maneuver which generally involves skipping outside the atmosphere. In this maneuver no control over the vehicle trajectory is available except that allowed by trimming the vehicle at a desired value of L/D prior to initiating re-entry. This value is then maintained throughout the reentry period.

DECELERATION LOADS

The undershoot boundary, generally the steepest allowable descent into the atmosphere, is generally defined from consideration of both aerodynamic heating and deceleration loads. It is assumed here that this boundary may be defined by man's tolerance to deceleration loading only since improved technology can alleviate the heating problem but can do little to increase man's ability to withstand high deceleration or "g" loads.

The maximum deceleration load obtained during reentry on a vehicle with $(L/D)_{max} = 1$ is presented in Figure 5 as a function of the initial reentry angle for several values of initial reentry velocity. It is assumed here that the crew can withstand no more than 12 g's without serious damage. This value then defines the undershoot boundary. The overshoot boundary, indicated by the dashed line, is presented to demonstrate the reduction in the reentry corridor with increasing velocity.

It is of interest to consider the maximum deceleration load obtained at this overshoot boundary. This gives the minimum "g" tolerance required by crew members to safely return from a space mission. These are shown in Figure 6 as affected by initial reentry velocity and vehicle lift-drag ratio capability. As is to be expected, increasing the vehicle L/D capability decreases the overshoot "g" load for a given value of initial velocity. Also, note that the maximum deceleration load at the overshoot boundary increases with increasing initial entry velocity. Therefore, if the undershoot boundary is "g" limited, a limiting velocity may be obtained where the undershoot and overshoot boundaries cross. For instance, if the undershoot boundary is defined by G_{max} = 12 g's, a limiting velocity of 93,300 fps is obtained for a vehicle having infinite lift-drag ratio capability. Thus, entry at velocities in excess of 93,300 fps is not possible unless man's tolerance to deceleration loads may be extended above 12 g's.

To further illustrate the reduction of maximum deceleration loads by increased vehicle L/D capability, G_{max} is presented in Figure 7 in terms of initial entry angle for vehicles re-entering the earth's atmosphere at escape speed (36,500 fps). As shown, the effect of increasing vehicle L/D capability is to reduce the maximum deceleration load for a given initial reentry angle. Maximum benefits occur by increasing L/D from 0 to 0.5 with little advantage to increasing a vehicle's lift-drag ratio capability above 1.

The comparitively high reentry velocities required by trips to the outer planets or "fast" trips to nearby planets may necessitate development of modulation techniques to reduce the peak "g" loads and achieve acceptable reentry corridor widths. One such method, originated by Grant, is presented in Figure 8. In this method, the vehicle is considered to operate on the illustrated drag polar where:

$$C_L = (C_{D_{max}} - C_{D_{min}}) \sin^2 \alpha \cos \alpha$$

and

$$C_D = C_{D_{min}} + (C_{D_{max}} - C_{D_{min}}) \sin^3 \alpha \tag{20}$$

In this method the vehicle initially operates at maximum lift coefficient. When the deceleration loads have reached a specified level, the angle of attack is modulated towards zero so as to maintain the deceleration load at a constant value. This results in a decreased value of G_{max} as is illustrated in Figure 8 for the particular case of a vehicle with $(L/D)_{max} = 1/2$ entering the atmosphere at escape speed. Modulation from $C_{L_{max}}$ to $(L/D)_{max}$ is seen to decrease G_{max} from 12.7 to 10 "g's" with only a slight effect on the altitude and range at pullout. A further reduction in peak "g" to 7 "g's" is attainable by modulation from $C_{L_{max}}$ to $C_{D_{min}}$. This greatly affects the ranging capability of the vehicle as indicated by the altitude-range curves of Figure 8. Increased modulation causes the vehicle to dig deeper into the atmosphere resulting in pullout at lower altitudes and velocities, thereby decreasing the vehicle's range capability.

Large increases in the reentry corridor width are attainable through the use of this technique of peak "g" reduction.

Reentry Corridor Width

Reentry corridor width is defined as the difference between the perigee altitudes of the overshoot and undershoot trajectories neglecting atmospheric effects and considering the earth as a point mass as shown by Figure 9. The overshoot and undershoot trajectories are thus simple conics defined by the initial entry velocity, V_i, and the angles γ_{i_o} and γ_{i_u}. The angles γ_{i_o} and γ_{i_u} are obtained by definition of the corridor boundaries for a particular vehicle lift-drag ratio and ballistic parameter, $\frac{W}{C_D A}$.

In the previous section it was stated that the undershoot boundary is defined by the maximum deceleration load attained during reentry. It is felt that G_{max} = 12 "g's" is a reasonable undershoot limit for manned reentry vehicles. Therefore, the undershoot boundary is defined as that trajectory for which a vehicle reentering the atmosphere with a positive value of L/D will receive a maximum deceleration load of 12 "g's".

It is much more difficult to define the overshoot boundary. However, for general purposes, it shall be defined as that trajectory for which the vehicle requires negative maximum lift capability to maintain constant altitude at the bottom of the pullout with initial entry at positive lift. Several other definitions will be discussed subsequently.

Utilizing the above boundary definitions, the overshoot and undershoot boundaries have been determined for a vehicle with $(L/D)_{max}$ = 1 and are shown in Figure 10. Here, overshoot and undershoot initial reentry angles are presented in terms of initial reentry velocity. Note that at satellite velocity $\gamma_{i_o} = 0°$ since the centrifugal force is initially equal to the vehicle weight requiring that the vehicle remain within the atmosphere. Also, a limit velocity of 83,000 fps (corresponding to zero corridor width) is obtained using the present boundary definitions.

The reentry corridor width may be indicated by the parameter, $\Delta\gamma_i = \gamma_{i_u} - \gamma_{i_o}$. The effect of vehicle L/D capability on this parameter is shown in Figure 11. As is to be expected, large gains in corridor width are obtained by increasing the vehicle L/D capability from 0 to 1. Note again that the limiting velocity is given by the initial reentry velocity for which $\Delta\gamma_i = 0$; and that safe entry is impossible for values of V_i greater than 93,300 fps under the constraints of the present corridor boundary definitions.

It is of interest to determine the effects of several boundary definitions on both the corridor boundaries and the actual corridor widths. Figures 12 and 13 illustrate such effects for a vehicle reentering the atmosphere at escape speeds. Three definitions of each boundary are considered. The undershoot boundaries are defined as follows:

+L/D, uncontrolled -- The vehicle enters the atmosphere with positive L/D and maintains constant L/D to pullout where a range control maneuver may be initiated.

Modulated, $C_{L_{max}}$ to $(L/D)_{max}$ -- The modulation technique discussed in Figure 8 is utilized to increase γ_{i_u}. The vehicle angle of attack may be modulated only from that for $C_{L_{max}}$ to that for $(L/D)_{max}$.

Modulated, $C_{L_{max}}$ to $C_L = 0$ -- The same as the above with the modulation capability extended to $C_L = 0$.

As shown, modulation greatly increases the undershoot entry angle and the benefits of this maneuver increase with increasing vehicle L/D capability. Note that without modulation the maximum benefits of increasing L/D are achieved at L/D = 1.

The overshoot boundaries are defined as follows:

+L/D, uncontrolled (h_{skip} = 400 mi.) -- The vehicle enters the atmosphere with positive L/D and maintains this value throughout the reentry period (no maneuver capability). A 400 mile maximum skip altitude is chosen as the limit so as to prevent penetration of the Van Allen radiation belts.

+L/D, controlled -- The vehicle enters the atmosphere with positive L/D and utilizes full negative lift capability to maintain constant altitude at the bottom of the pullout.

$-C_{L_{max}}$ -- The vehicle enters the atmosphere with full negative lift capability and barely remains within the atmosphere. This is the absolute limit for wholly atmospheric re-entry maneuvers.

The +L/D, uncontrolled overshoot boundary is shown to be impractical for significant values of L/D (L/D > .2). The other two definitions show little variation with lift-drag ratio with the $-C_{L_{max}}$ definition yielding approximately 1/2 degree more corridor width than the +L/D, controlled definition.

A design reentry corridor should have flexible boundaries capable of extension for emergency reentry conditions. Therefore, the overshoot boundary is generally taken as the +L/D, controlled case and the undershoot boundary as the +L/D, uncontrolled case.

The midcourse guidance and control required for a space mission is specified by a combination of system guidance and control capabilities and reentry vehicle corridor width capabilities. Since system guidance and control capability is essentially an engineering or "hardware" problem, we shall be concerned in this study only with the vehicle corridor width capability.

The actual reentry corridor widths corresponding to the boundary definitions of Figure 12 are presented in Figure 13 for an initial entry velocity of 36,500 fps. At this reentry velocity the maximum corridor width for the +L/D, uncontrolled case is about 15 miles and becomes zero for a value of L/D = .475. Therefore, the vehicle must be controlled at the overshoot boundary for safe reentry of vehicles with significant L/D capability. Modulation at the undershoot boundary is seen to significantly increase corridor width. This method will be required at the high entry velocities associated with short interplanetary trips to insure sufficient reentry corridor widths from the guidance and control standpoint. Note also that by choosing the +L/D, controlled definition for the overshoot boundary, an additional 10 miles of corridor is maintained in reserve for emergency conditions wherein the $-C_{L_{max}}$ entry made may be utilized.

Increasing the reentry velocity above escape velocity results in decreasing corridor widths. Eventually, the point of zero corridor width will be reached. A combination of propulsive and aerodynamic braking will be required for such high initial reentry velocities.

RANGE CONTROL

Longitudinal

Range control is achieved by aerodynamic maneuvers initiated after pullout to zero flight path angle. A reentry vehicle must be capable of reaching the desired landing site after initial reentry from any point within the reentry corridor. That is, the maximum range attainable by the vehicle entering the atmosphere at the undershoot boundary must be at least equal to the minimum range attainable by entry at the overshoot boundary. In addition, some range overlap (see Figure 14) is desirable to offset errors in initial reentry time since time errors introduce range errors due to the earth's rotation. The degree of range overlap required is of course defined by the allowable mission time errors and the angle of the reentry plane with respect to the equatorial plane.

Before proceeding with a discussion of the range overlap capabilities of reentry vehicles, it is desirable to consider the longitudinal range capabilities of a vehicle carrying out the aerodynamic maneuvers of Figure 4.

The range attainable by the constant L/D reentry maneuver is shown in Figure 15 for an initial velocity of 36,500 fps (escape speed). The boundaries considered in this figure are a 10g undershoot boundary and a 400 mile skip overshoot boundary. Range control is obtained by selecting the appropriate L/D for a given initial reentry angle. The slope of the lines of constant L/D indicate that large errors in range would occur for small errors in setting the trim angle of attack (reentry L/D). Note also that, for these boundary conditions, safe reentry is not available for values of L/D greater than .475. These limitations in range control and usable vehicle L/D demonstrate that control over the reentry trajectory must be utilized for the safe reentry and landing of a manned vehicle returning from a space mission at escape or higher speeds.

It thus becomes necessary to consider the longitudinal range attainable by the controlled atmospheric maneuvers of Figure 4. As an illustrative example we shall consider return from a lunar mission with a reentry vehicle having a maximum L/D capability of 1/2. The longitudinal ranges attainable by this vehicle throughout the reentry corridor are presented in Figure 16. An entry angle of -5.25° represents the overshoot boundary and 7.6°, the undershoot boundary. The two limiting curves represent essentially the limiting ranges of which the vehicle is capable. The maximum range curve is obtained by utilizing a constant altitude maneuver at the bottom of the initial reentry pullout. Constant altitude is maintained until sufficient kinetic energy has been dissipated such that, if a constant L/D = 1/2 trajectory is then initiated, the vehicle will skip outside the atmosphere to a maximum altitude of 400 miles. This maximum range maneuver is, however, critically dependent on the velocity and path angle at which the skip is initiated. Therefore, this maneuver is considered to be too susceptible to large uncorrectable range errors to be a reliable method of range control. The greatest range attainable by a wholly atmospheric maneuver is given by the equilibrium glide curve, which gives ranges of about 6,000 miles near the undershoot boundary. This appears adequate for return from the lunar mission. The constant altitude curve is obtained by maintaining constant altitude at the bottom of the pullout for as long as possible. As shown, quite short ranges are obtained at the undershoot boundary. The minimum indicated ranges were obtained by the use of a constant 10 "g" deceleration load maneuver.

The range overlap for this vehicle and mission varies from 400 to 12,000 miles depending on the maximum range maneuver utilized. The equilibrium glide maneuver, yielding 4,000 miles range overlap, is probably the best operational maneuver.

The effect of increasing the initial reentry velocity on the longitudinal range overlap is presented in Figure 17. Here, the maximum range is obtained by the constant altitude maneuver and the minimum range by the constant "g" maneuver. The trends would be the same for the equilibrium glide maneuver although this maneuver is not considered here. As shown, increasing either the initial reentry velocity or the vehicle L/D capability yields an increased range overlap. Both results are to be expected. One effect of increasing velocity is to bring the corridor boundaries closer together, thus the initial maneuver conditions are more nearly the same for the maximum and minimum range maneuvers. The effect of increasing the vehicle L/D capability yields increased maneuverability and hence, longer ranges. Of course, this increased range overlap with increased reentry velocity may be offset by the increased range overlap requirements of the deep space missions associated with these reentry velocities.

It is necessary to determine the ability of pilots to fly the maneuvers of interest. Many pilot simulation studies have been carried out in an effort to define optimum methods of pilot control over the reentry trajectory. The ranges attainable by some of these are shown in Figure 18 for reentry at escape speed of a vehicle with a maximum L/D capability of 1/2. The reentry guidance and control techniques considered are: the reference trajectory technique, the repetitive prediction technique, and the pilot controlled technique. In the reference trajectory procedure the control feedbacks were developed for successful operation of the system. The repetitive prediction system utilized a rapidtime analog computer to predict the range capability from the present conditions. The pilot's intelligence and learning capabilities were used to provide the guidance logic and the control commands in the pilot controlled technique.

The repetitive prediction technique was shown to yield very good control of the initial peak deceleration and, hence, minimal ranges. The maximum range maneuver utilized here for the simulator studies is an arbitrary maneuver wherin a pull-up, initiated upon entering the atmosphere, is terminated at an altitude of approximately 250,000 feet with a velocity of about 26,000 ft/sec. This flight plan is most nearly approximated by the equilibrium glide maneuvers of the present study, indicated by the dashed line on Figure 18. The piloted maximum ranges are shown to be much less than the theoretical values. It appears, however, that with further system refinement and pilot schooling, ranges quite close to the theoretical values may be obtained.

Lateral

Significant lateral range capability is required of a vehcile returning from a deep space mission since the reentry plane angle may vary considerably from the nominal due to mid-course guidance corrections. In addition, time errors may introduce large lateral range requirements if the reentry plane is not the equatorial plane.

A vehicle's lateral range capability may be shown to increase with increasing entry velocity. Therefore, determination of a vehicle with sufficient L/D capability to satisfy lateral range requirements for reentry at satellite velocity will apply for reentry at all higher velocities. The effect of the vehicle's maximum L/D capability on its lateral range capability is shown in Figure 19 for entry at satellite velocity. Lateral range is seen to increase rapidly with L/D capability reaching 1/4 the earth's circumference at an L/D of about 3.5. This is the maximum lateral range capability which could be required since a vehicle reentering the atmosphere in the equatorial plane could reach either of the poles. Similarly, a vehicle reentering in a polar plane could reach any point on the earth by proper combination of the vehicle lateral and longitudinal range capabilities. A vehicle's design lateral range capability will, of course, depend on the allowable range errors introduced by the space vehicle's guidance and control systems.

As an example of the L/D required from the lateral range standpoint, let us consider reentry from a polar orbit. The range required to reach a particular landing site either once or twice daily is presented in Figure 20. Also shown is the L/D required. Return to the continental United States may be accomplished twice daily by a vehicle with L/D of approximately 0.9. Thus, the particular mission requirements are seen to reduce the L/D required for lateral range from 3.5 to 0.9. This effect of specific mission requirements reducing the lateral range requirements may be expected to hold for the deep space missions with high reentry velocities. It cannot be stated at the present time exactly what lateral range capability will be required for reentry at high velocities. Therefore, no attempt is made here to define specific lateral range capabilities or requirements for these missions.

AERODYNAMIC HEATING

Convective

Aerodynamic heating is the heating of a reentry vehicle due to the friction of the air as the vehicle passes through it. It may be divided into two components: convective and radiative. Convective heating is the dominant source of heating at the lower reentry velocities with radiative heating becoming the dominant source at the higher velocities.

The convective stagnation point heating rate equation may be written approximately as:

$$\dot{q}_c = \frac{K \sqrt{\rho}\, V^{3.15}}{\sqrt{R_n}} \tag{21}$$

where ρ = atmospheric density

V = velocity

R_n = vehicle nose radius

The total stagnation point convective heat load is obtained by integration of equation (15) over the reentry time period. Note that convective heating is inversely proportional to the square root of the vehicle nose radius. For this reason, reentry vehicles operating in the range of entry velocities where convective heating dominates have blunt nose shapes. Notable examples are the Mercury, Gemini, and Apollo vehicles.

Since a knowledge of the vehicle shape is required for a complete heating analysis, we are concerned here only with the stagnation point heating loads so as to maintain the generality of the study. The stagnation point heating is quite sufficient to indicate the effects of vehicle L/D capabilities, reentry velocities, and atmospheric maneuvers on the aerodynamic heating problem. In particular, design of a reentry vehicle heat shield is dependent on the maximum heating rates and total heat loads expected to be encountered during reentry. These are, of course, the stagnation point values.

The effect of the particular atmospheric maneuver utilized during reentry on the maximum heating rate and total heat load is presented in Figure 21 for a vehicle with L/D = 1/2 reentering the earth's atmosphere at escape speed. Since all the maneuvers considered here are initiated after pullout, the same value of maximum heating rate and maximum "g" load apply to each maneuver for the same initial reentry conditions. As is to be expected, the minimum range, constant "g" maneuver yields minimum total heat loads for a given initial entry condition. The maximum range, constant L/D, skipping maneuver yields the greatest total heat loads. Note that maximum total heat loads occur at the overshoot boundary with low values of $\dot{q}_{c_{max}}$ while minimum total heat loads and high values of $\dot{q}_{c_{max}}$ occur at the undershoot boundary. This is due to the fact that at the undershoot boundary the vehicle dips deeper into the atmosphere into regions of higher atmospheric density than at the overshoot boundary. Since the vehicle is in a higher density region when the maneuver is initiated, it will, of course, dissipate its kinetic energy much faster than at the overshoot boundary resulting in lower total heat loads.

The maximum convective heating rates (undershoot) and the maximum convective total heat loads (overshoot) are presented in Figures 22 and 23 to demonstrate the effects of vehicle L/D capability and initial reentry velocity on these quanities. The expected results of increasing maximum heating rates and total heat loads with increasing vehicle L/D capability or initial reentry velocity are obtained. Increasing L/D capability yields increased values of $\dot{q}_{c_{max}}$ since the vehicle resultant force coefficient is reduced thereby causing the undershoot boundary pullout to occur at lower altitudes (higher density) for the same initial reentry velocity and angle. Increased total heat loads result due to the increased maneuverability of the higher L/D vehicle. Increased initial reentry velocity yields increased heating rates since the heating rate is more velocity dependent than density dependent as shown by equation (15). Also, the total heat load is increased due primarily to the greater kinetic energy of the higher velocity vehicles which must be dissipated within the atmosphere.

Obviously, the convective heating problem becomes more severe as more sophisticated space missions are undertaken.

Radiative

The radiative stagnation point heating rate equation may be written approximately as:

$$\dot{q}_r = K\rho^r V^s R_n \qquad (22)$$

where the exponents r and s are dependent on the velocity regime in which the vehicle is flying. Radiative heating is considered to be negligibly small at velocities less than 25,000 fps and approaching that required to dissipate the entire kinetic energy at high velocities. Note that the radiative stagnation point heating is directly proportional to the vehicle nose radius. This indicates that pointed shapes are optimum from the radiative heating standpoint. Thus, once again, the designer is faced with a tradeoff problem. The vehicle nose shape must be designed from consideration of both convective and radiative heating and is quite mission dependent.

The total heat loads as obtained for a vehicle with a one foot nose radius and a maximum L/D capability of one are presented in Figure 24 for two types of entry: maximum L/D and maximum lift coefficient. This figure indicates the superiority of entry at maximum lift coefficient from consideration of heating only. Of course, operation at $C_{L_{max}}$ results in a loss of corridor width and range capability since the vehicle is operating at a value of L/D less than the maximum value.

Of particular interest is the role played by radiative heating. For the case shown here, radiative heating is negligible in comparison to convective heating for initial entry velocities less than about 45,000 fps. As the reentry velocity is increased however, radiative heating quickly becomes the dominant heating factor. Therefore a completely different vehicle design is required for a reentry velocity of 70,000 fps than for a reentry velocity of 40,000 fps.

CONCLUDING REMARKS

A

The major problems in reentry--deceleration loads, corridor width, range control, and heating loads--have been discussed. The effects of reentry vehicle L/D capability, initial reentry velocity, and atmospheric maneuvers on these problems have been demonstrated. No clear cut conclusions may be drawn here since the only intention has been to bring to the reader a better knowledge of what is meant by the word "reentry". Also, it has been the purpose here to point out the complexities of designing a reentry vehicle.

The effect of increased L/D capability was shown to be advantageous from the standpoint of corridor width, deceleration loads, and range control, but most disadvantageous from the standpoint of aerodynamic heating. The role played by vehicle nose shape in reentry has been demonstrated by the opposing effects of convective and radiative heating. The necessity for a vehicle to have the capability of maneuvering within the atmosphere was shown. The effect of initial reentry velocity was to indicate that in all probability a specific reentry vehicle must be defined for each space mission or reentry velocity range. Thus, the trend of the past--the Mercury vehicle for the orbital mission and the Apollo vehicle for the lunar mission--will probably be continued in the future. Increased L/D capability will be demanded by the more stringent requirements of reentry at the hyperbolic velocities associated with interplanetary missions. Finally, propulsion may well be required to slow a vehicle returning from fast interplanetary trips to velocities for which the vehicle may safely reenter the atmosphere.

APPENDIX A

SYMBOLS

A	vehicle reference area
C_D	drag coefficient
C_L	lift coefficient
$C_{L_{e.g.}}$	lift coefficient used during the equilibrium glide maneuver
D	drag
g	gravitational acceleration
h	altitude
L	lift
L/D	lift-drag ratio
m	vehicle mass
R	longitudinal range
R_c	radius of curvature of reentry flight path
r	radial distance from earth center
r_e	earth radius
t	time
V	velocity
W	vehicle weight
α	angle of attack
γ	reentry angle
ρ	atmospheric density

BIBLIOGRAPHY

1. Adams, Mac C.: A Look at the Heat Transfer Problem at Super-Satellite Speeds. Preprint 1556-60, ARS, Dec., 1960.

2. Allen, H. J.: Problems in Atmospheric Entry from Parabolic Orbits. Paper presented at Conference on Aeronautical and Space Engineering. Nagoya, Japan. Nov. 8-9, 1960.

3. Allen, H. Julian, and Eggers, A. J., Jr.: A Study of the Motion and Aerodynamic Heating of Ballistic Missiles Entering the Earth's Atmosphere at High Supersonic Speeds. NASA Report 1381, 1958.

4. Anon.: Lift Entry of Manned Space Vehicles: Generalized Determination of the Aerodynamics and Thermodynamics Associated with the Lift-Vector Modulation Technique. Douglas Report SM-42120, Douglas Aircraft Co., Inc., Aug. 1962.

5. Baradell, D. L.: A Look at the Reentry Problem. NASA Report 63-318, Aug. 1963.

6. Baradell, D. L.: Lateral Range Control by Banking During Initial Phases of Supercircular Reentries. NASA TN D-1511, 1962.

7. Baradell, D. L., and McLellan, C. H.: Lateral Range and Hypersonic Lift-Drag Ratio Requirements for Efficient Ferry Service from a Near-Earth Manned Space Station. Paper presented at Second Manned Space Flight Meeting, Dallas, Texas, April, 1963.

8. Becker, John V.: Heating Penalty Associated with Modulated Entry into Earth's Atmosphere. ARS Journal, May, 1960. pp. 404-405.

9. Becker, John V.: Re-Entry from Space. Scientific American, Vol. 204, No. 1, Jan. 1961, pp. 51-57.

10. Becker, J. V., Baradell, D. L., and Pritchard, E. B.: Aerodynamics of Trajectory Control for Reentry at Escape Speed. Paper presented at the International Academy of Astronautics Symposium, Paris, France. June 1961. Also published in Astronautica Acta, Vol. VII, Fasc. 5-6, 1961. pp. 334-358.

11. Bell, Richard W., and Hung, Francis C. S.: Implications of Reentry Trajectory Control on Vehicle Design Criteria at Superorbital Speeds. Society of Automotive Engineering Inc. National Aerospace Engineering and Manufacturing Meeting. Los Angeles, Calif. Oct. 8-12, 1962.

12. Boissevain, Alfred G.: The Effect of Lateral- and Longitudinal-Range Control on Allowable Entry Conditions for a Point Return From Space. NASA TN D-1067, 1961.

13. Broglio, L.: Similar Solutions in Re-Entry Lifting Trajectories. Univ. of Rome, SIARgraph No. 54, Dec. 1959.

14. Bryant, J.,P., and Frank, M. P.: Supercircular Reentry Guidance for a Fixed L/D Vehicle Employing a Skip for Extreme Ranges. Paper presented at ARS Lunar Missions Meeting, Cleveland, Ohio, July 1962.

15. Bryson, A. E., and Denham, W. F.: A Guidance Scheme for Supercircular Reentry of a Lifting Vehicle. Paper presented at ARS Space Flight Report to the Nation, Oct. 1961.

16. Bryson, A. E., Denham, W. F., Carroll, F. J., and Mikami, K.: Determination of the Lift or Drag Program That Minimizes Reentry Heating With Acceleration or Range Constraints Using a Steepest Descent Computation Procedure. Presented to the IAS 29th Annual Meeting, New York, Jan. 23-25, 1961.

17. Chapman, Dean R.: An Approximate Analytical Method for Studying Entry Into Planetary Atmospheres. NASA TR R-11, 1959.

18. Chapman, D. R.: An Analysis of the Corridor and Guidance Requirements for Supercircular Entry Into Planetary Atmospheres. NASA TR R-55, 1959.

19. Cheatham, Donald C., Young, John W., and Eggleston, John M.: The Variation and Control of Range Traveled in the Atmosphere by a High-Drag Variable-Lift Entry Vehicle. NASA TN D-230,1960.

20. Detra, R. W., Riddell, F. R., and Rose, P. H.: Controlled Recovery of Non-Lifting Satellites. AVCO Report 54, May 1959.

21. Eggers, Alfred J., Allen, H. Julian, and Neice, Stanford E.: A Comparative Analysis of the Performance of Long-Range Hypervelocity Vehicles. NACA Report 1382, 1958.

22. Eggleston, John M., and Young, John W.: Trajectory Control for Vehicles Entering the Earth's Atmosphere at Small Flight-Path Angles. NASA TR R-89, 1961.

23. Foudriat, Edwin C.: Study of the Use of Terminal Controller Techniques for Reentry Guidance of a Capsule-Type Vehicle. NASA TN D-828, 1961.

24. Foudriat, Edwin C., and Wingrove, Rodney C.: Guidance and Control During Direct-Descent Parabolic Reentry. NASA TN D-979, 1961.

25. Galman, B. A.: Direct Re-entry at Escape Velocity. Paper presented at Third Annual Meeting, American Astronautical Society, Seattle, Washington, Aug. 8-11,1960.

26. Grant, Frederick C.: Dynamic Analysis of a Simple Reentry Maneuver for a Lifting Satellite. NASA TN D-47, 1959.

27. Grant, Frederick C.: Importance of Variating of Drag With Lift in Minimization of Satellite Entry Acceleration. NASA TN D-120, 1959.

28. Grant, Frederick C.: Analysis of Low-Acceleration Lifting Entry From Escape Speed. NASA TN D-249, 1960.

29. Grant, Frederick C.: Modulated Entry. NASA TN D-452, 1960.

30. Grazley, Carl, Jr.: Deceleration and Heating of a Body Entering a Planetary Atmosphere From Space. Rand Report P-955, 1957.

31. Hayes, J. E., Rose, P. H., and Vander Velde, W. E.: Analytical Study of a Drag Brake Control System for Hypersonic Vehicles. WADD Tech. Report. 60-267, Jan. 1960.

32. Hildebrand, R. B.: Manned Reentry at Super-Satellite Speeds. IAS Paper No. 60-83, June 1960.

33. Hildebrand, R. B.: Manned Return From Space. Presented at the Sec. Internat. Congress of Aero. Sciences, Zurich, Switzerland, Sept. 1960.

34. Jackson, Charlie M., Jr.: Estimates of Minimum Energy Requirements for Range-Controlled Return of a Nonlifting Satellite From a Circular Orbit. NASA TN D-980, 1961.

35. Katzen, Elliot D., and Levy, Lionel L., Jr.: Atmosphere Entries with Vehicle Lift-Drag Ratio Modulated to Limit Deceleration and Rate of Deceleration - Vehicles With Maximum Lift-Drag Ratio of 0.5. NASA TN D-1145, 1961.

36. Knip, Gérald, Jr., and Zola, Charles L.: Three-Dimensional Trajectory Analysis for Round-Trip Missions to Mars. NASA TN D-1316, 1962.

37. Knip, Gerald, Jr., and Zola, Charles L.: Three-Dimensional Sphere-of-Influence Analysis of Interplanetary Trajectories to Mars. NASA TN D-1199, 1962.

38. Lees, Lester: Re-entry Heat Physics. Astronautics, March 1959, pp.22-23.

39. Lees, Lester, Hartwig, Frederic W., and Cohen, Clarence B.: Use of Aerodynamic Lift During Entry Into the Earth's Atmosphere. ARS Journal, Vol. 29, No. 9, 1959, pp. 633-641.

40. Levy, Lionel L., Jr.: An Approximate Analytical Method for Studying Atmosphere Entry of Vehicles With Modulated Aerodynamic Forces. NASA TN D-319, 1960.

41. Levey, Lionel L., Jr.: The Use of Drag Modulation to Limit the Rates at Which Deceleration Increases During Nonlifting Entry. NASA TND-1037, 1961.

42. Love, Eugene S.: Reentry Vehicles: General Concepts and Operational Modes. Reentry Dynamics. Bulletin of Virginia Polytechnic Institute, Eng. Station Ser. No. 150, Vol. LV, No. 10, Aug. 1962.

43. Love, Eugene S., and Pritchard, E. Brian: A Look at Manned Entry at Circular to Hyperbolic Velocities. Paper presented at AIAA Second Manned Space Flight Meeting, Dallas, Texas, April 22-24, 1963.

44. Luidens, Roger W.: Approximate Analysis of Atmospheric Entry Corridors and Angles. NASA TN D-590, 1961.

45. Luidens, Roger W.: Flight-Path Characteristics for Decelerating From Supercircular Speed. NASA TN D-1091, 1961.

46. Mandell, D. S.: A Study of the Manuevering Performance of Lifting Re-Entry Vehicles. Paper presented at ARS 15th Annual Meeting, Washington, D.C., Dec. 5-8, 1960.

47. Morth, R.: Reentry Trajectory Perturbations From Adjoint Equations. Boeing Doc. D2-5294, Jan. 1960.

48. Morth, Raymond, and Speyer, Jason: Control Systems for Supercircular Entry Maneuvers. The Boeing Company. Presented at the IAS 30th Annual Meeting, New York, New York, Jan. 22-24, 1962. IAS Paper No. 62-3.

49. Morth, Raymond, and Speyer, Jason: Divergence From Equilibrium Glide Path at Super Satellite Velocities. Jour. of the Am. Rocket Soc., March 1961.

50. Morth, R.: Optimum Re-entry Trajectories by Dynamic Programing. Boeing Document D2-9748, April 1961.

51. Moul, Martin T. Schye, Albert A., and Williams, James L.: Dynamic Stability and Control Problems of Piloted Reentry From Lunar Missions. NASA TN D-986, 1961.

52. Price, Donald A., Jr., Kepler, Don I., and Krop, Martin A.: Configuration Concepts for Earth Reentry From Planetary Missions. LMSC A 031360, 1963.

53. Pritchard, E. Brian: Aerodynamic Control of Deceleration and Range for the Lunar Mission. Paper presented at SAE National Aeronautics Meeting, New York, New York, April 3-6, 1962.

54. Pritchard, E. Brian: Longitudinal Range Attainable by the Constant-Altitude Variable-Pitch Reentry Maneuver Initiated at Velocities up to Escape Velocity. NASA TN D-1811, 1963.

55. Roberts, Leonard: Ablation Materials for Atmospheric Entry. Proceedings of the NASA-University Conference on the Science and Technology of Space Exploration, Vol. 2, Chicago, Ill., Nov. 1962.

56. Robinson, Alfred C., and Besonis, Algimantas, J.: On the Provlems of Re-Entry Into the Earth's Atmosphere. WADC Technical Report 58-408, Aug. 1958.

57. Rose, Peter H.: Reentry From Lunar Missions. Preprint No. 7, Lunar Flight Symposium, American Astronautical Society, Denver, Colo., Dec. 29, 1961.

58. Rose, Peter H.: Future Problems in Reentry Pgysics. Paper presented at Second Manned Space Flight Meeting, Dallas, Texas, April 22-24, 1963.

59. Rosenbaum, R.: Longitudinal Range Control for a Lifting Vehicle Entering a Planetary Atmosphere. Presented at ARS Guidance, Control, and Navigation Conf. Aug. 7-9, Paper 1911-61.

60. Scala, S. M.: Heating Problems of Entry Into Planetary Atmospheres From Supercircular Orbiting Velocities. General Electric Space Sciences Laboratory, R61SD176, 1961.

61. Schmidt, D.: Ablative Thermal Protection for Aerospace Vehicles. WADD TN 61-48, March, 1961.

62. Schwaniger, Auther J.: Use of Lift for Deceleration and Range Control for Re-Entry of Space Vehicles. Army Ballistic M Missile Agency Report No. DS-TM-39-60, May 11, 1960.

63. Shahan, R. L.: Reentry Guidance for Manned Space Craft. Paper presented at ARS IRE 15th Annual Tech. Con., April 1961.

64. Slye, Robert E.: An Analytical Method for Studying the Lateral Motion of Atmosphere Entry Vehicles. NASA TN D-325, 1960.

65. Sommer, Simon C., and Short, Barbara J.: Point Return From a Lunar Mission for a Vehicle that Maneuvers Within the Earth's Atmosphere. NASA TN D-1142, 1961.

66. Smith, R. H., and Menard, J. A.: Supercircular Entry and Recovery With Maneuverable Manned Vehicles. Aerospace Engineering, October, 1961.

67. Styler, E. F.: A Parametric Examination of Re-Entry Vehicle Size and Shape for Return at Excape Velocity. Paper presented at Third Annual Meeting, American Astronautical Society, Seattle, Washington, Aug. 8-11, 1960.

68. Styler, Eugene F., and Zimmerman, Donald K.: Thermal Protection Structure for Lifting Super-Orbital Entry. Preprint IAS No. 62-103, June 1962.

69. Swann, Robert T.: Composite Thermal Protection Systems for Manned Reentry Vehicles. ARS Journal, Vol. 32, No. 2, Feb. 1962, pp. 221-226.

70. Teagur, R.: Flight Mechanics of Re-Entry After Circumlunar Flight by Means of Various Lifting Techniques. NASA George C. Marshall Space Flight Center, MNN-M-Aero-4-60 (Sept. 15, 1960).

71. Ting, Lu: Some Aspects of Drag Reduction for Lifting Wing-Body Combinations at Supersonic Speed. PIBAL Report No. 445, May 1958.

72. Trimpi, Robert L., Grant, Frederick C., and Cohen, Nathaniel B.: Aerodynamic and Heating Problems of Advanced Reentry Vehicles. Proceedings of the NASA-University Conference on the Science and Technology of Space Exploration, Vol.2, Chicago, Ill., Nov. 1962.

73. Wang, H. E., and Chu,S. T.: Variable Lift Re-Entry at Super-Orbital and Orbital Speeds. AIAA Journal, Vol. I, No. 5, May 1963.

74. Wang, K., and Ting, L.: Analytic Solutions of Planar Re-Entry Trajectories With Lift and Drag. Polytechnic Institute of Brooklyn. (PIBAL) Report No. 601 (April 1960).

75. Wick, Bradfore H.: Radiative Heating of Vehicles Entering the Earth's Atmosphere. Paper presented at the AGARD Specialists' Meeting at T.C.E.A. Rhode-Saint-Genese, Belgium, April 1962.

76. Wingrove, Rodney C.: A Survey of Atmosphere Guidance and Control Methods. Presented at the IAS 31st Annual Meeting, New York, New York, Jan. 21-22, 1963. IAS Paper No. 63-86.

77. Wingrove, Rodney C., and Coate, Robert E.: Piloted Simulator Tests of a Guidance System Which Can Continuously Predict Landing Point of a Low L/D Vehicle During Atmospheric Re-Entry. NASA TN D-787, 1961.

78. Wong, Thomas J., and Slye, Robert E.: The Effects of Lift on Entry Corridor Depth and Guidance Requirements for the Return Lunar Flight. NASA TR R-80, 1960.

79. Young, John W.: A Method of Longitudinal and Lateral Range Control for a High-Drag Low-Lift Vehicle Entering the Atmosphere of a Rotating Earth. NASA TN D-954, 1961.

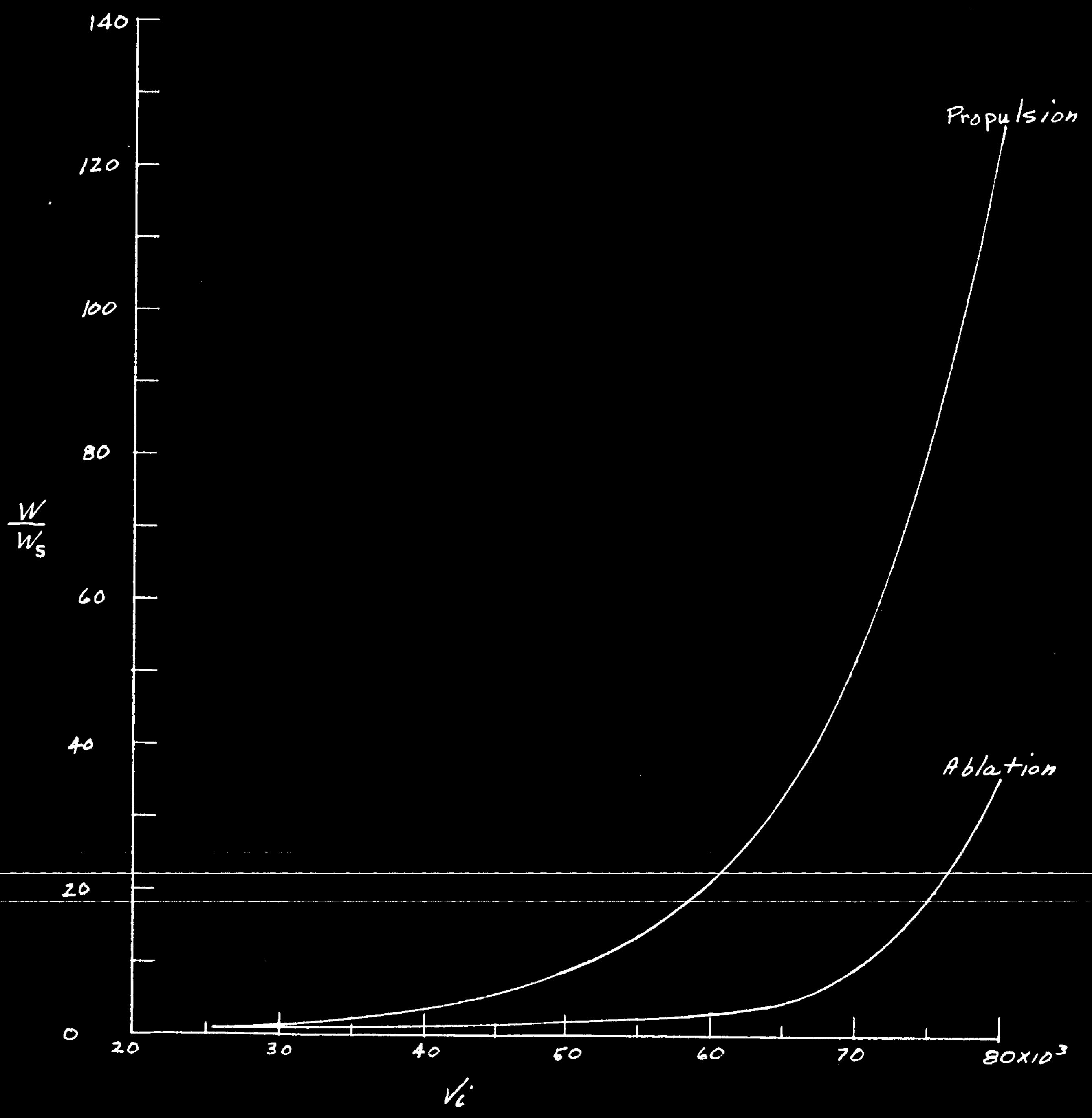

Figure 1. - Comparison of rocket and aerodynamic braking.

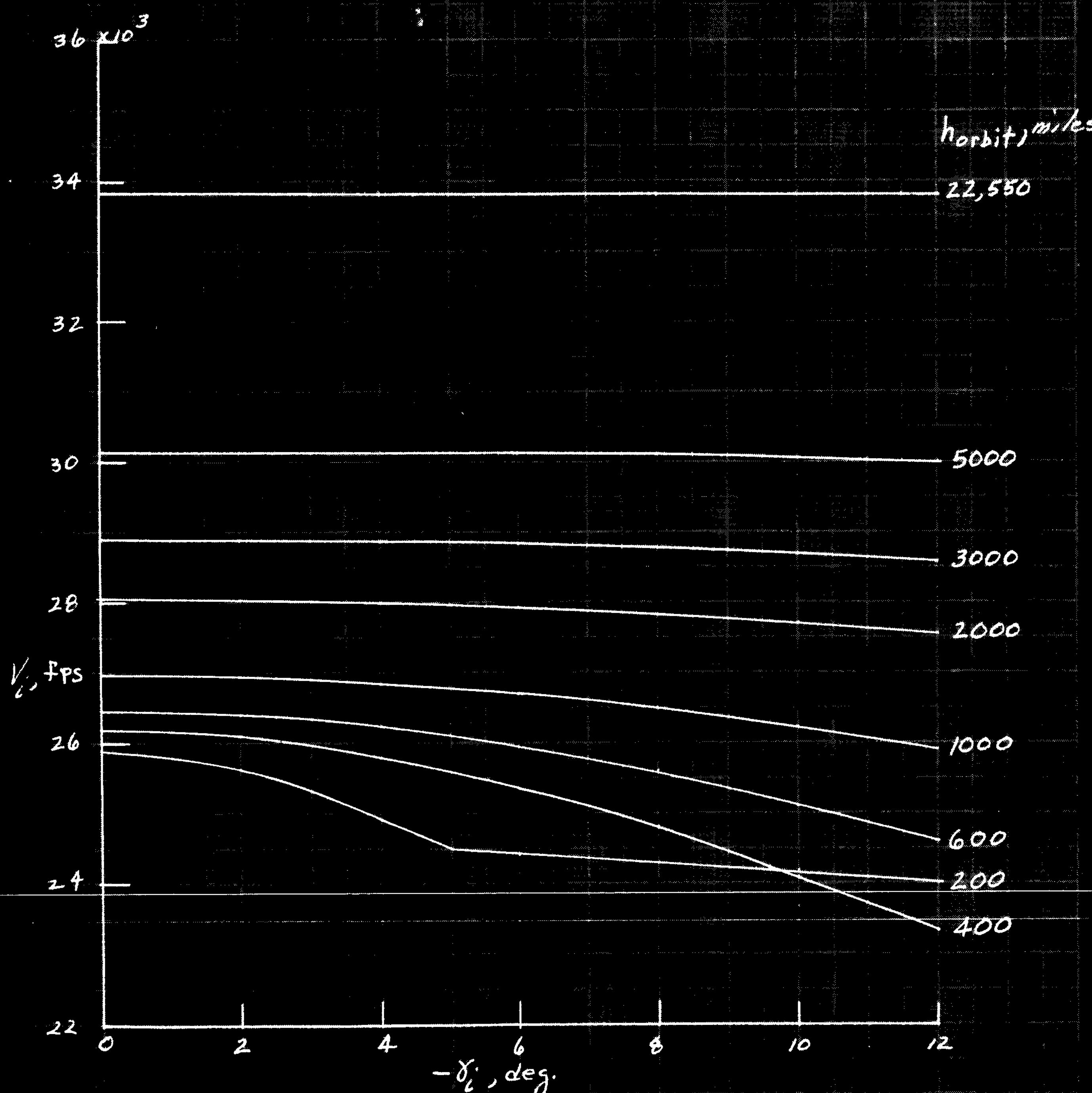

Figure 2. - Reentry velocity and angle for return from a circular orbit.

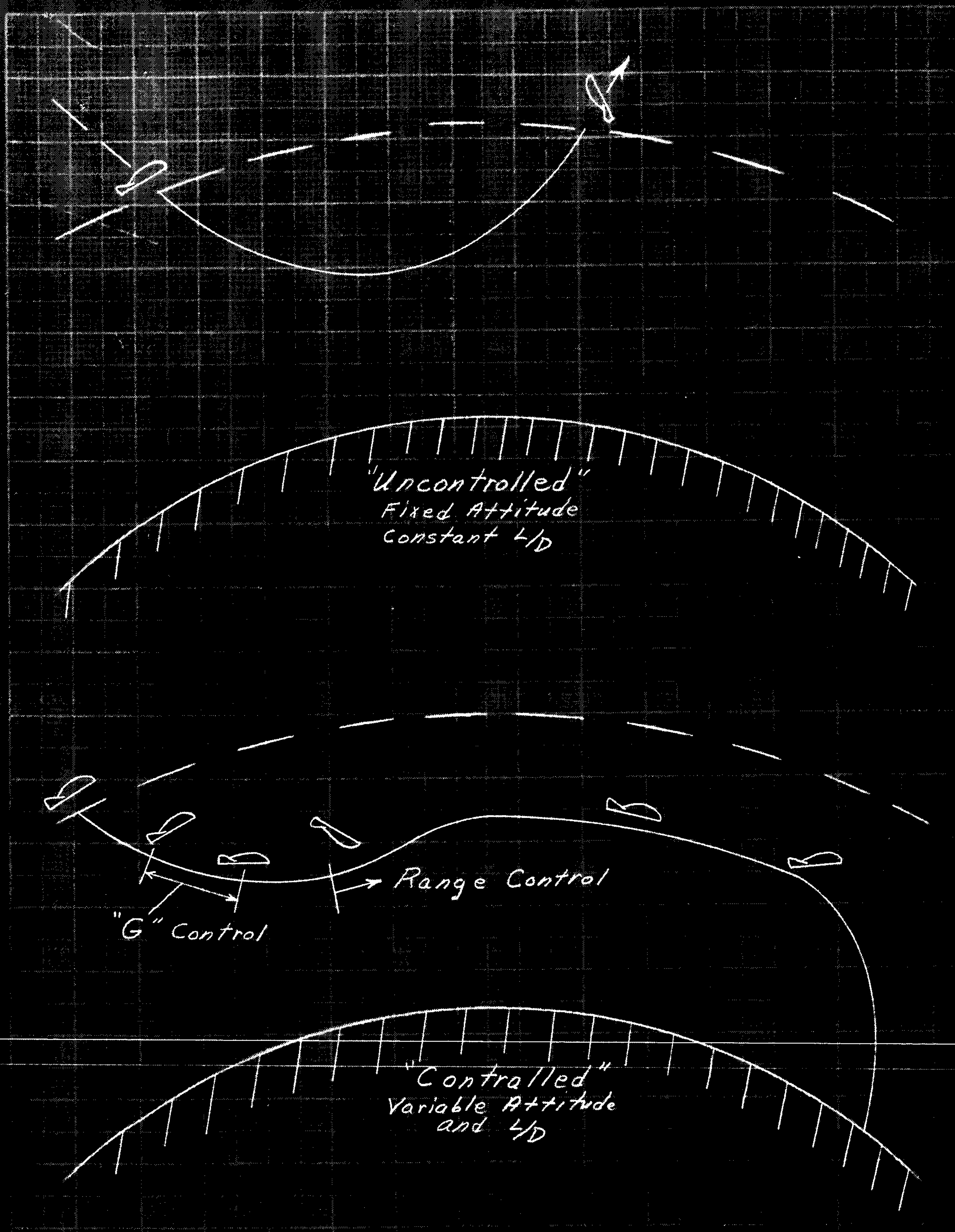

Figure 3. - Comparison of "uncontrolled and "controlled" reentry.

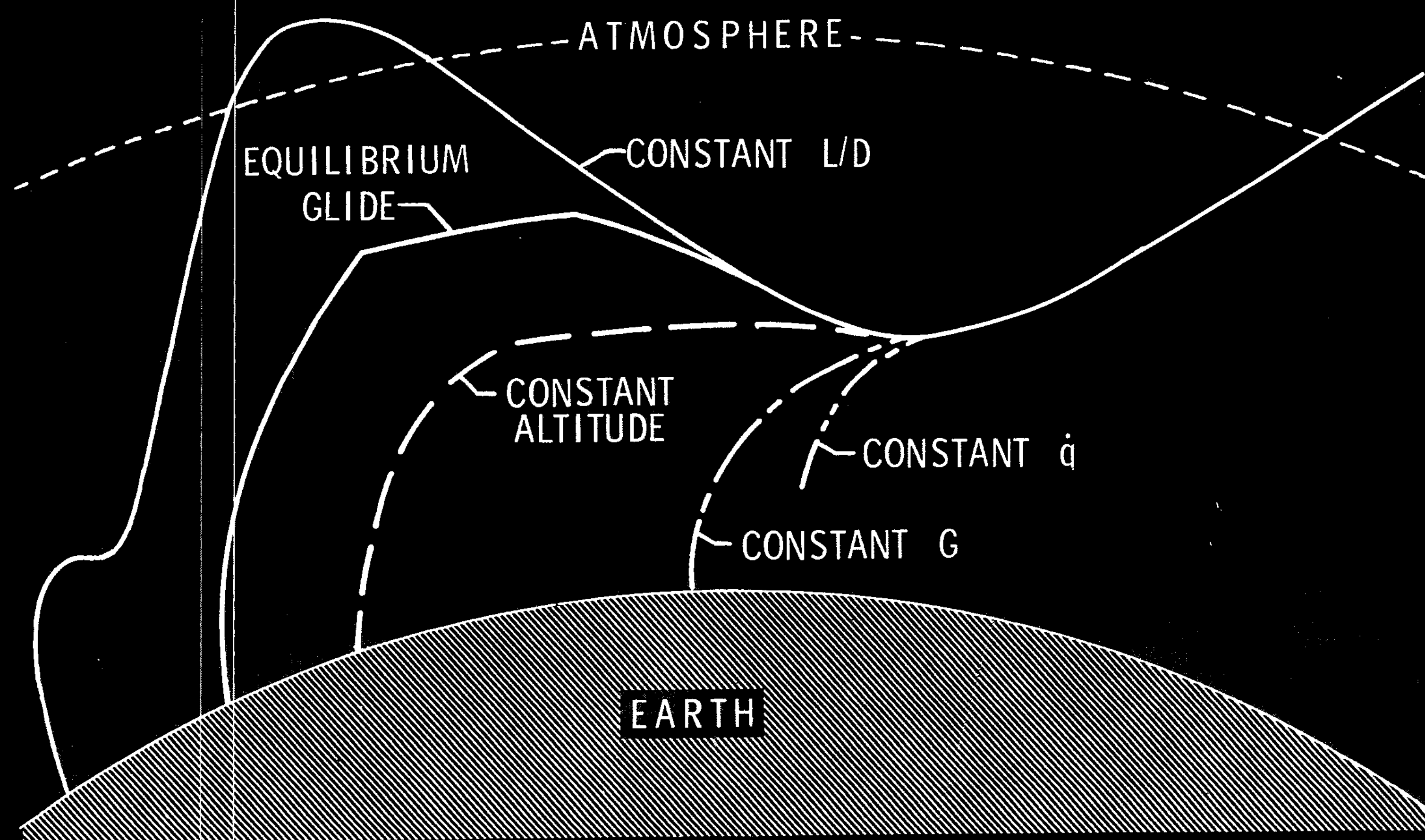

Figure 4. - Atmospheric maneuvers.

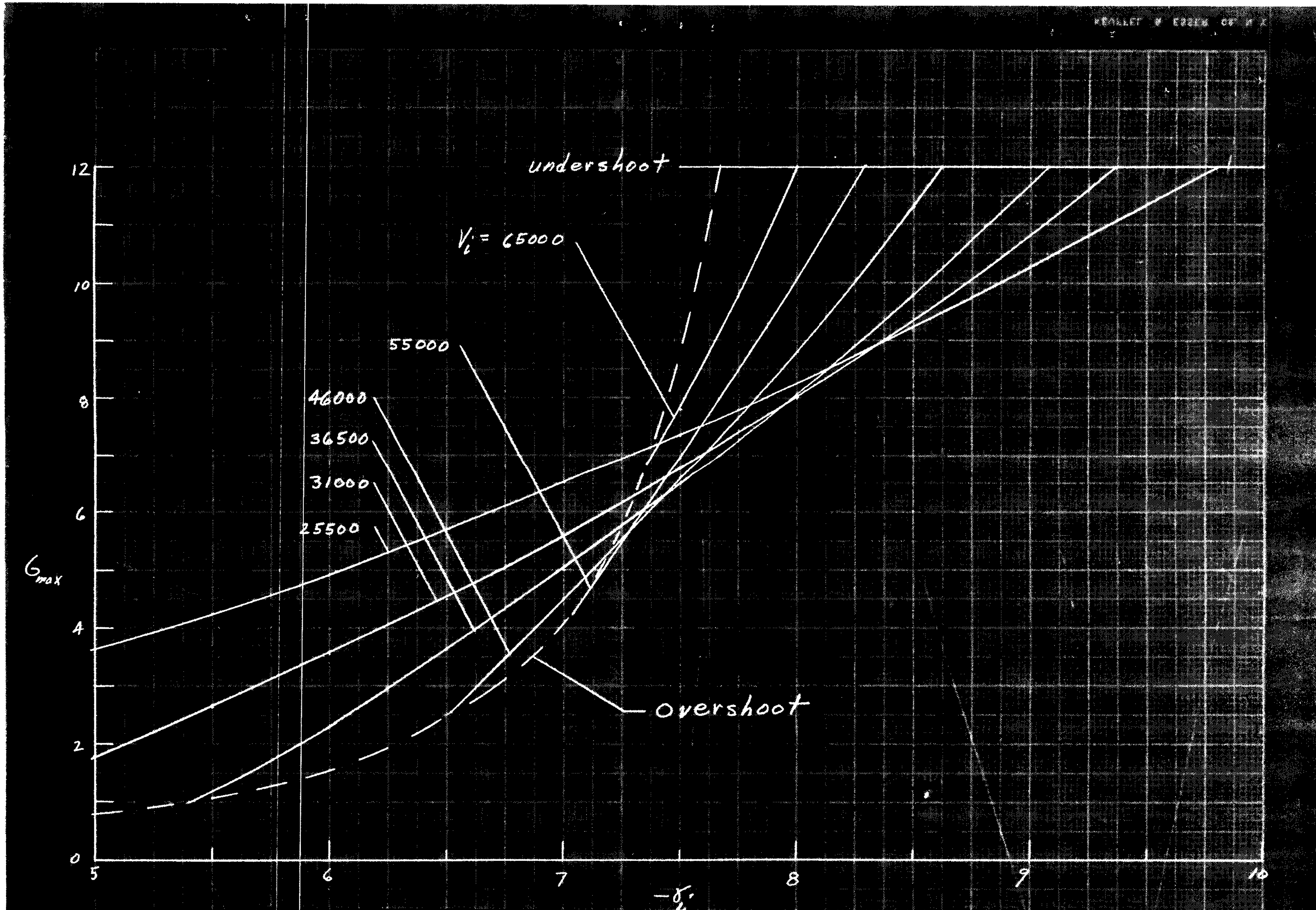

Figure 5. - Maximum deceleration loads. $(L/D)_{max} = 1.0$.

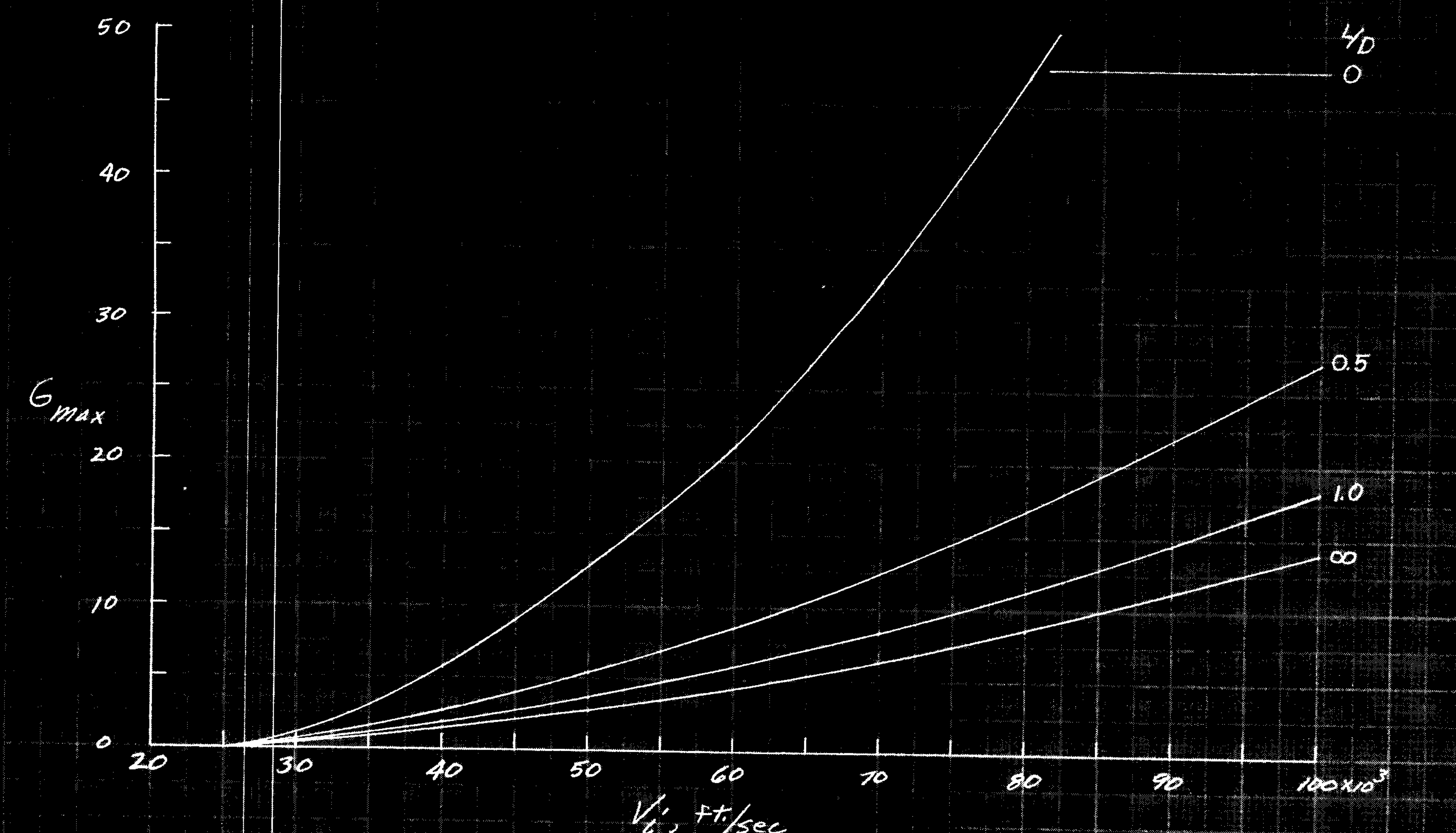

Figure 6. - Maximum deceleration load at the overshoot boundary.

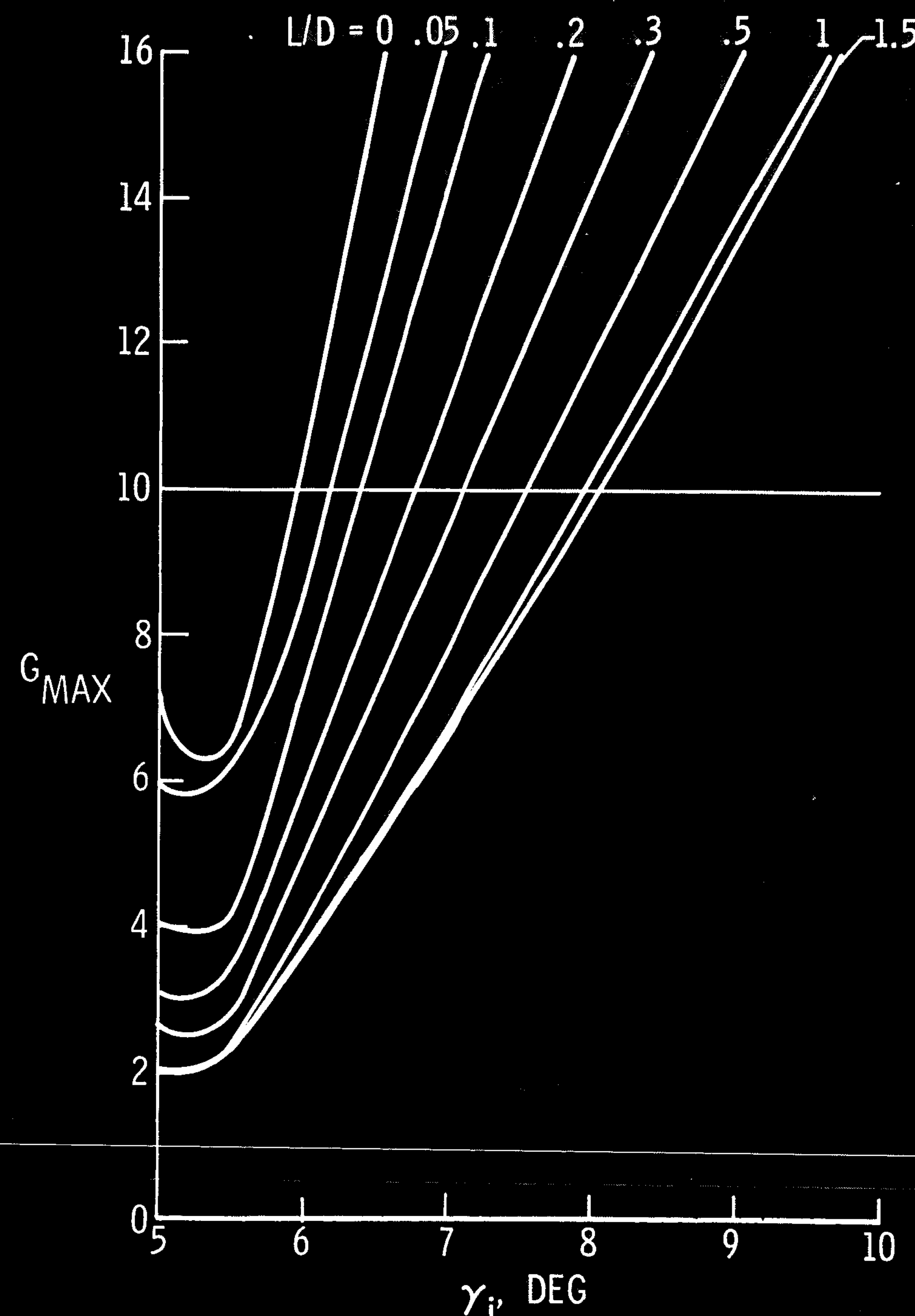

Figure 7. - Effect of vehicle L/D capability in maximum deceleration loads. (V_i = 36,500 fps).

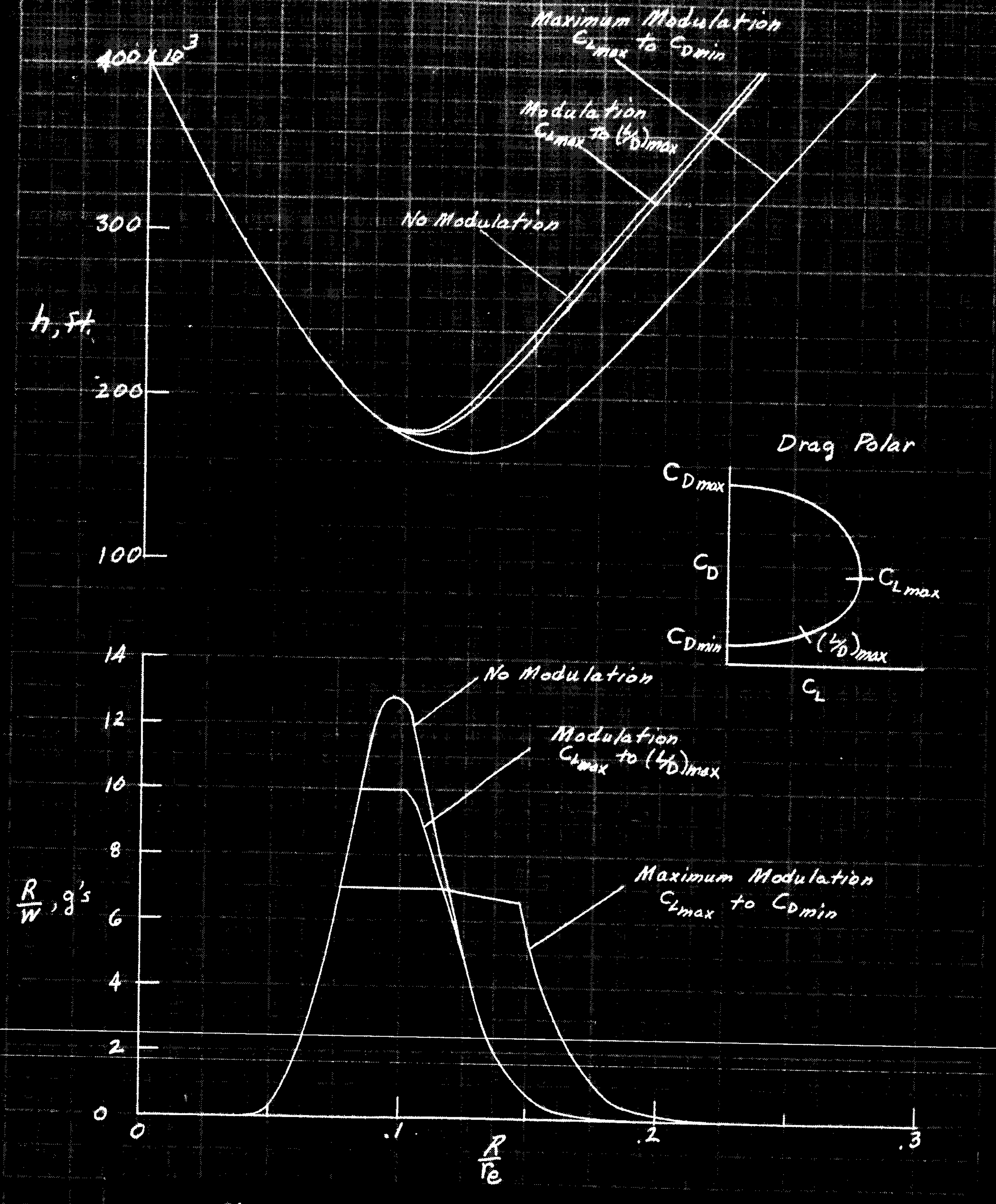

Figure 8. - Modulated reentry technique.
$\gamma_i = -8.11^\circ$.
$V_i = 36{,}500$ fps.

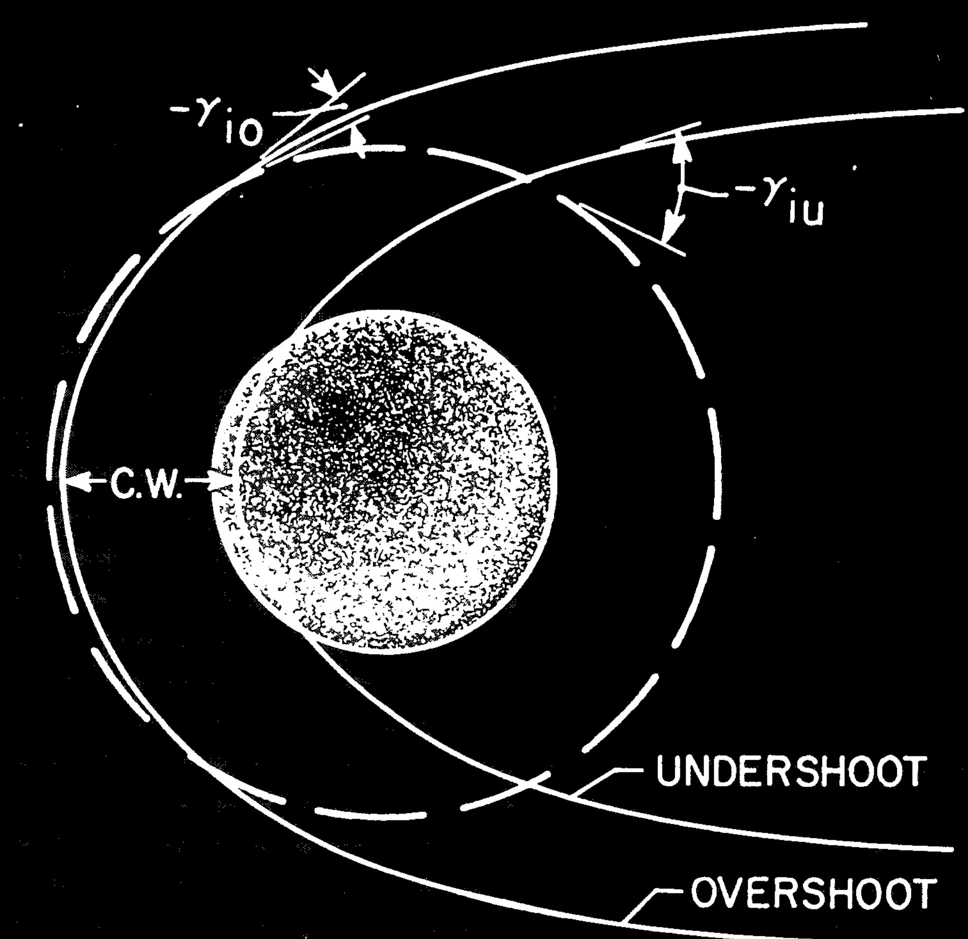

Figure 9. - Reentry corridor width.

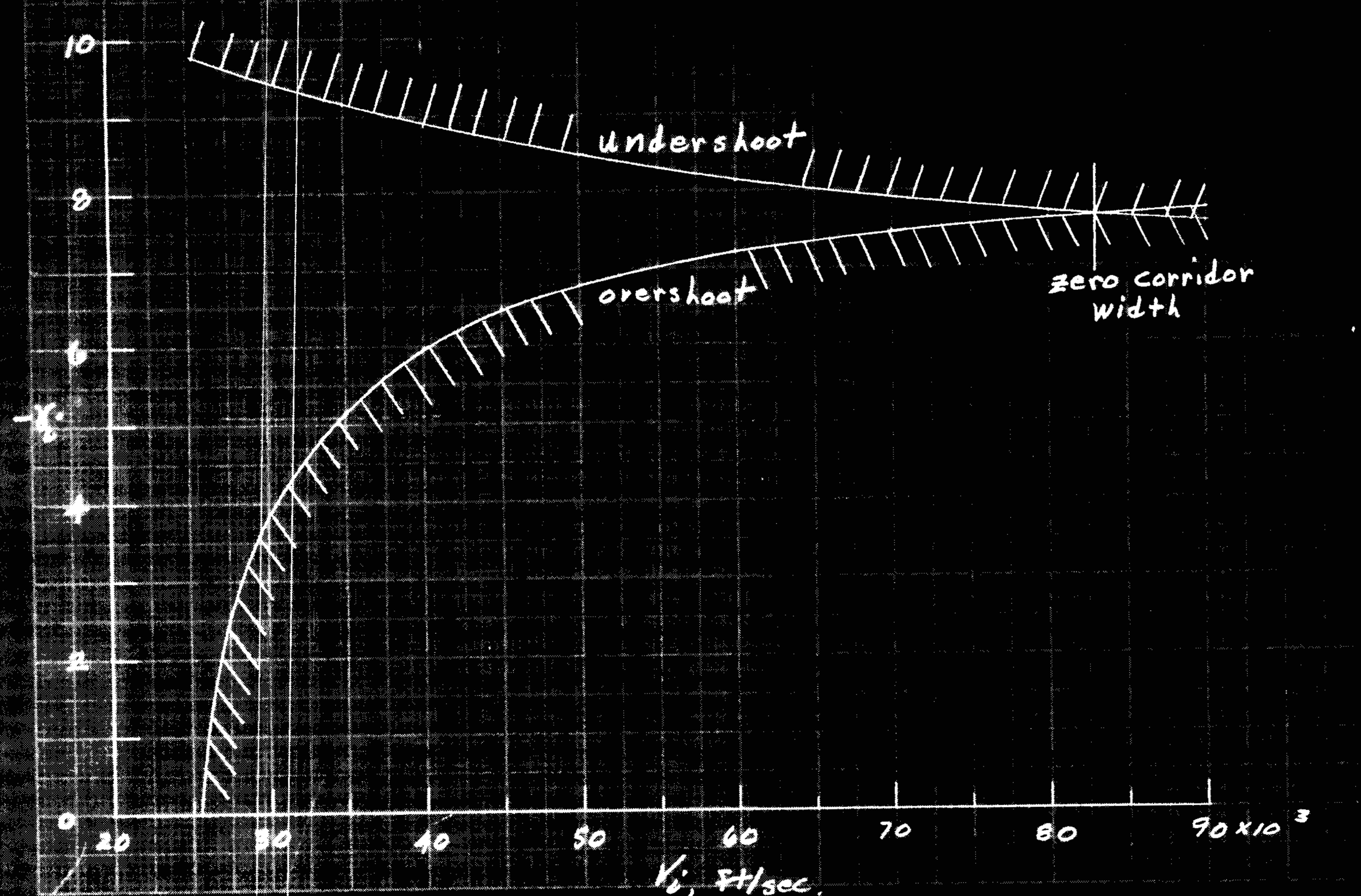

Figure 10. - Effect of initial reentry velocity on the reentry corridor boundaries. $((L/D)_{max} = 1.0)$

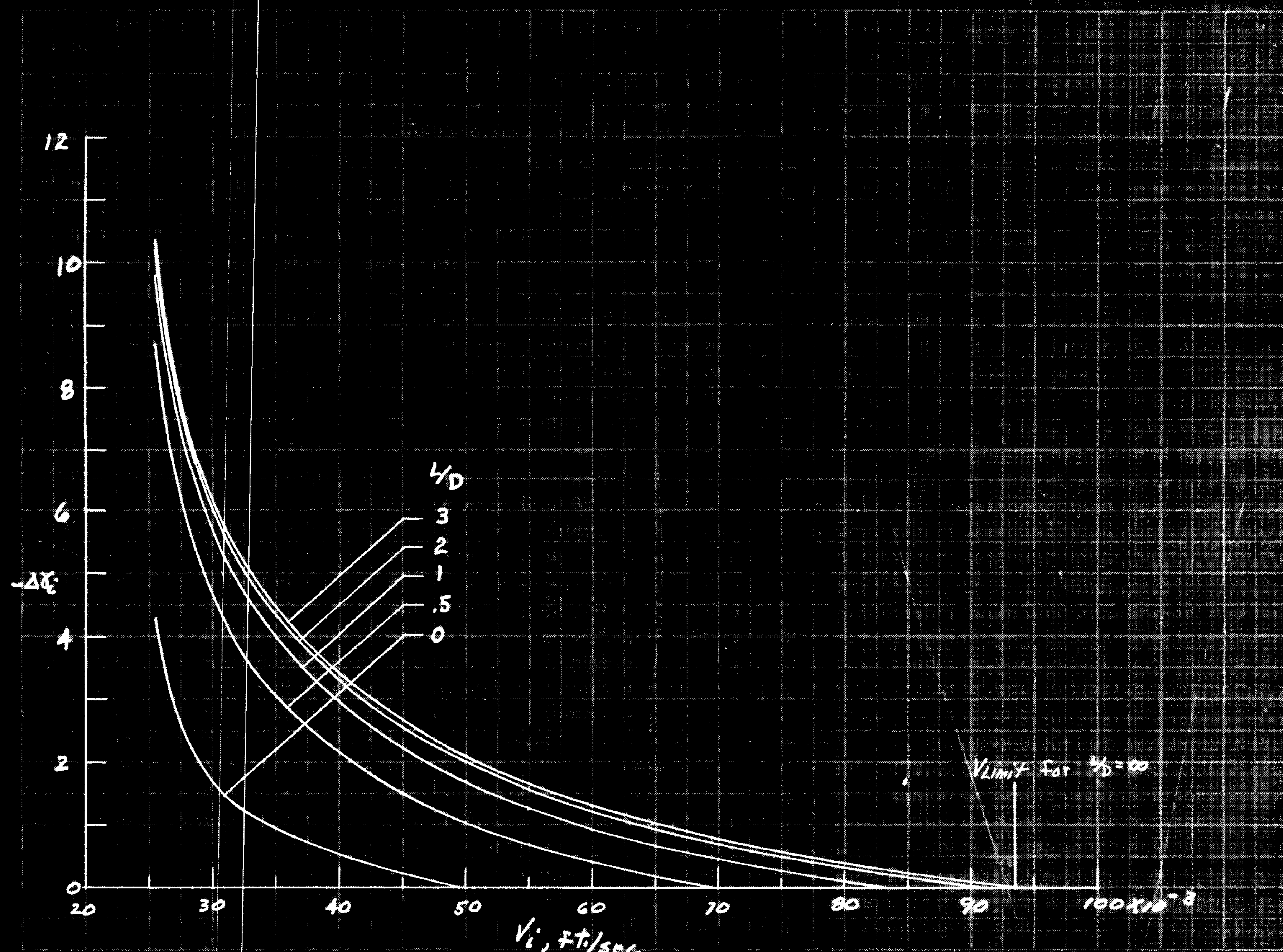

Figure 11. - Effect of initial reentry velocity on the reentry corridor width.

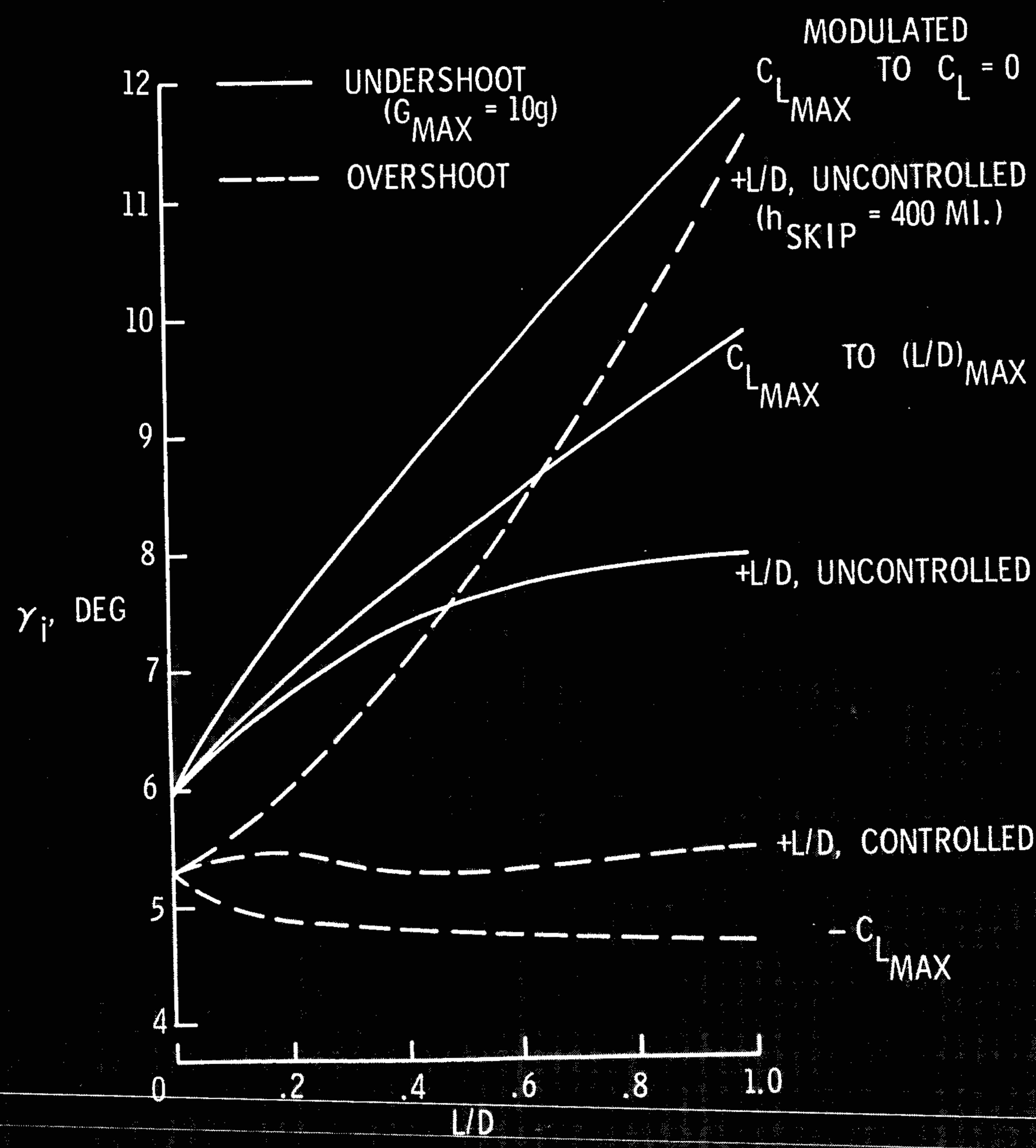

Figure 12. - Effect of vehicle L/D capability and atmospheric maneuvering on the reentry corridor boundaries. (V_i = 36,500 fps)

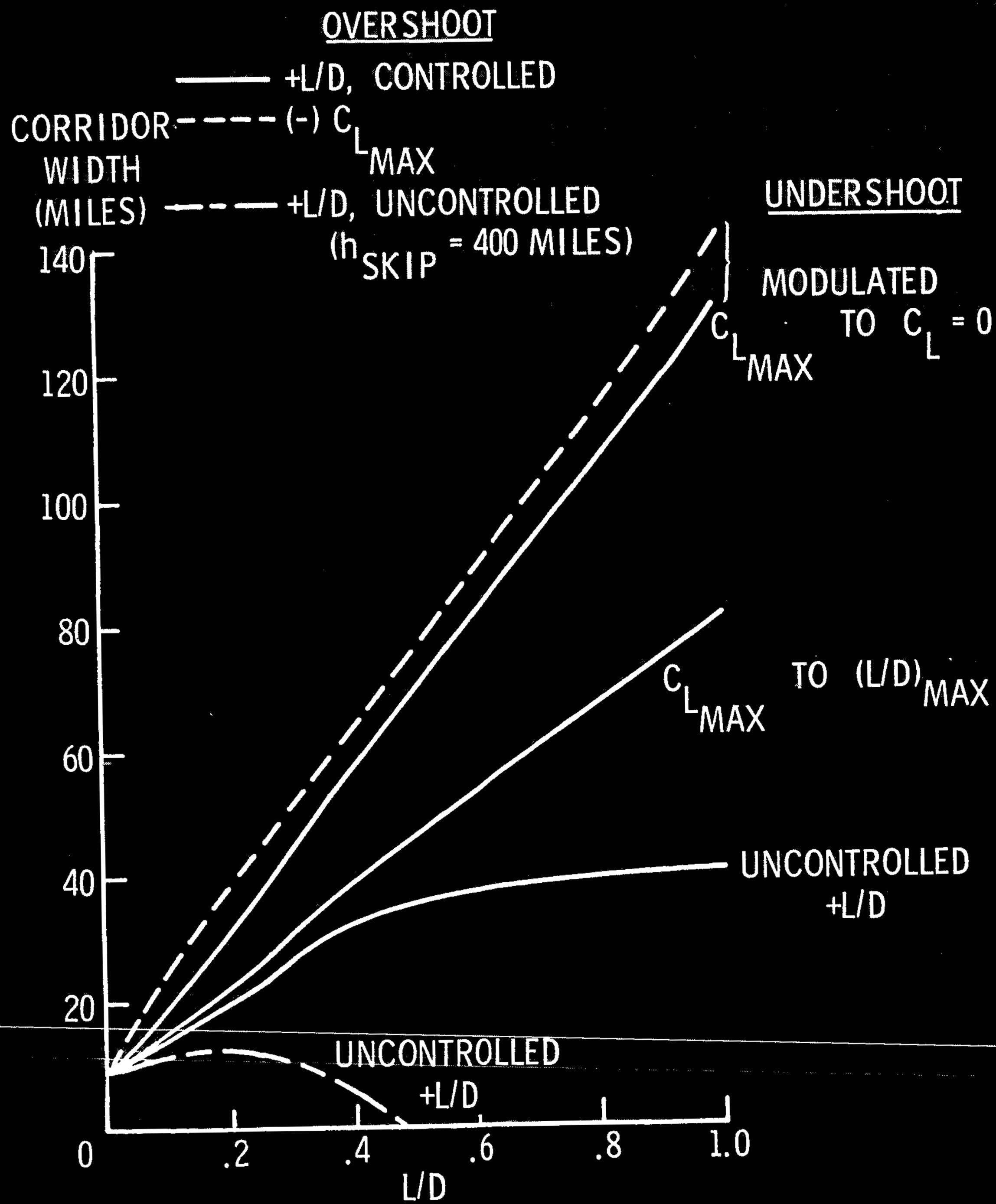

Figure 13. - Effect of vehicle L/D capability and atmospheric maneuvering on the reentry corridor width.
(V_i = 36,500 fps)

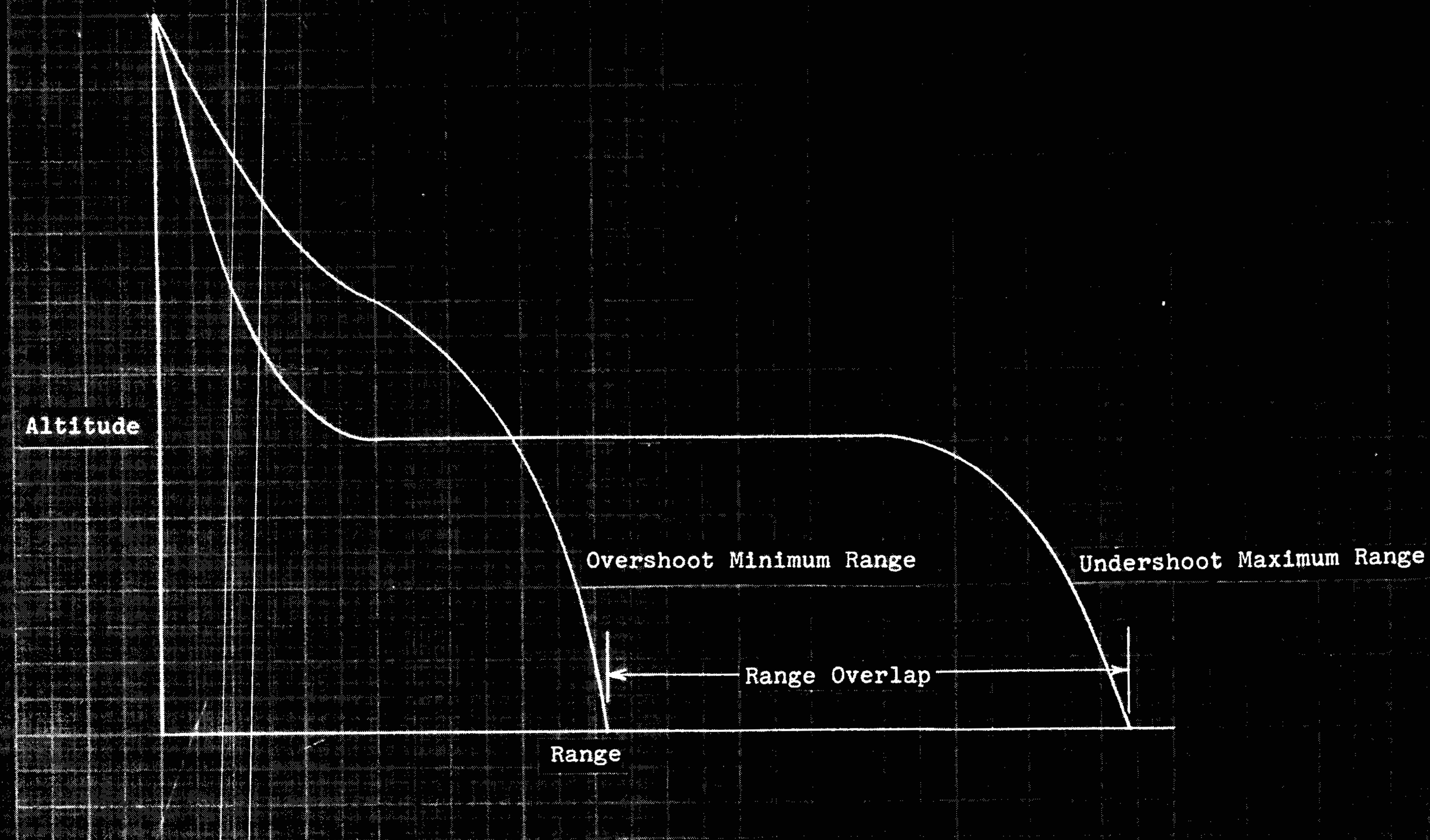

Figure 14. - Longitudinal range overlap.

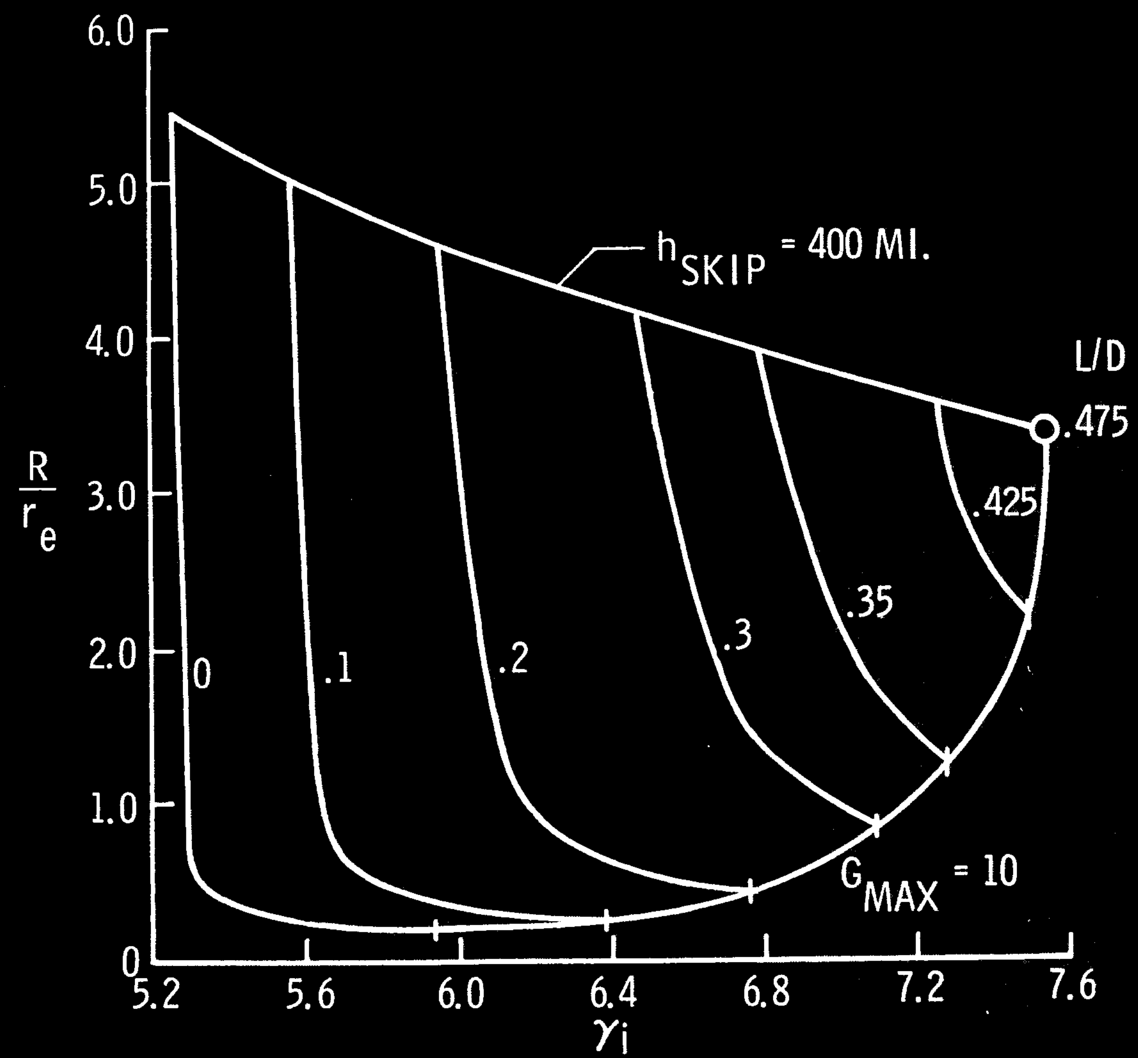

Figure 15. - Longitudinal range attainable by the constant L/D maneuver. V_i = 36,500 fps

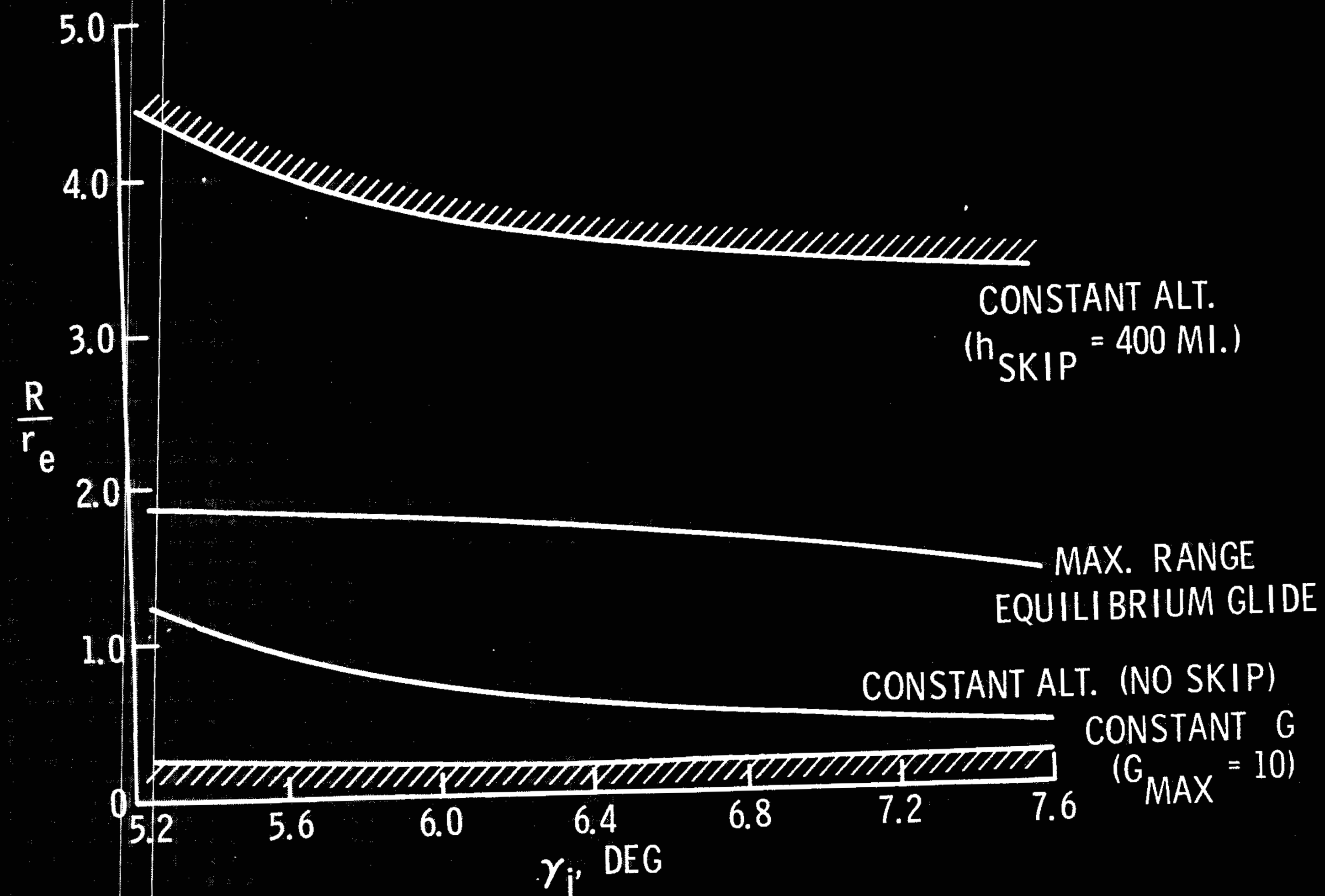

Figure 16. - Effect of atmospheric maneuver on attainable longitudinal range. ($L/D = 1/2$, $V_i = 36{,}500$ fps)

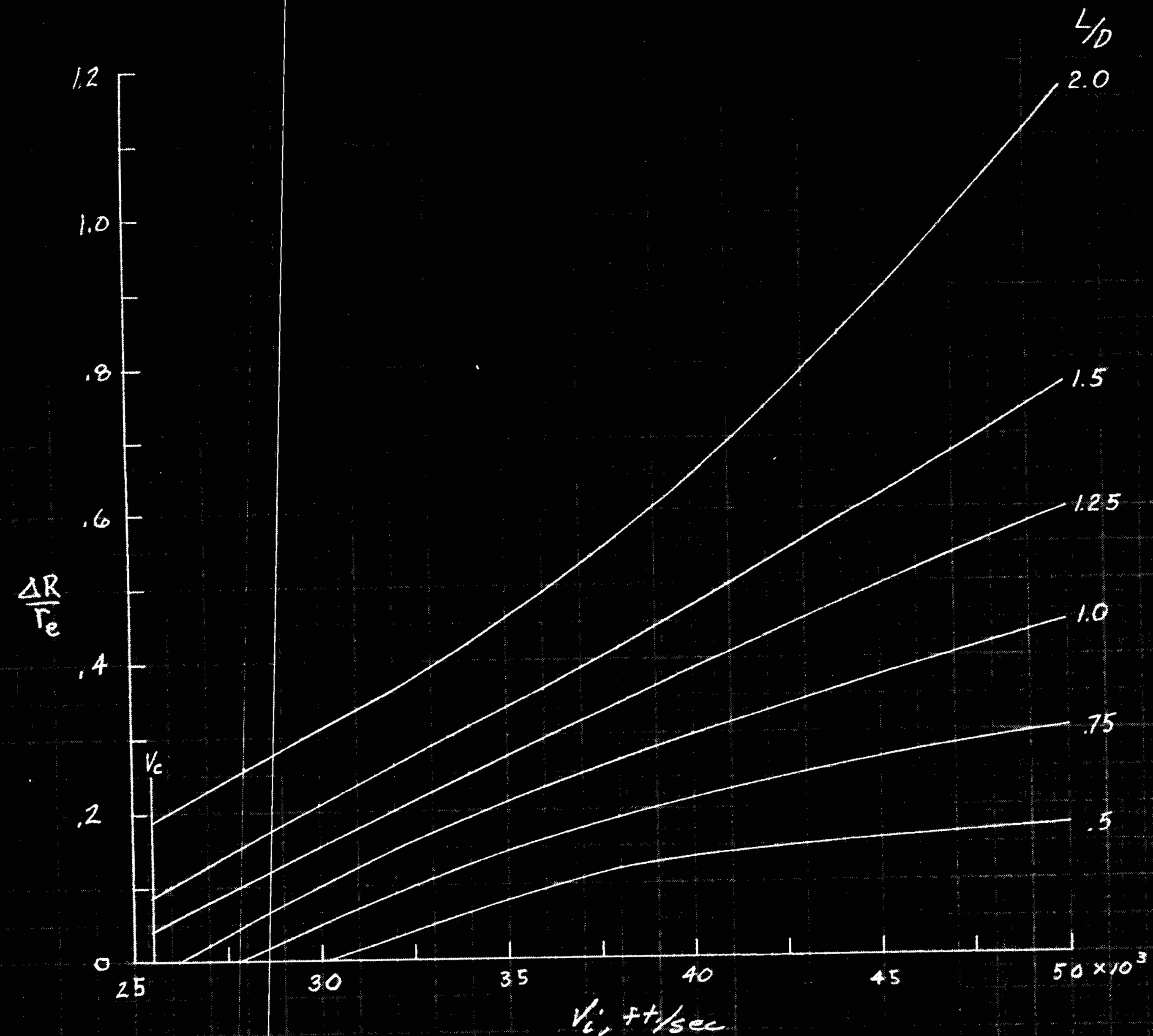

Figure 17. - Effect of initial reentry velocity on longitudinal range overlap.

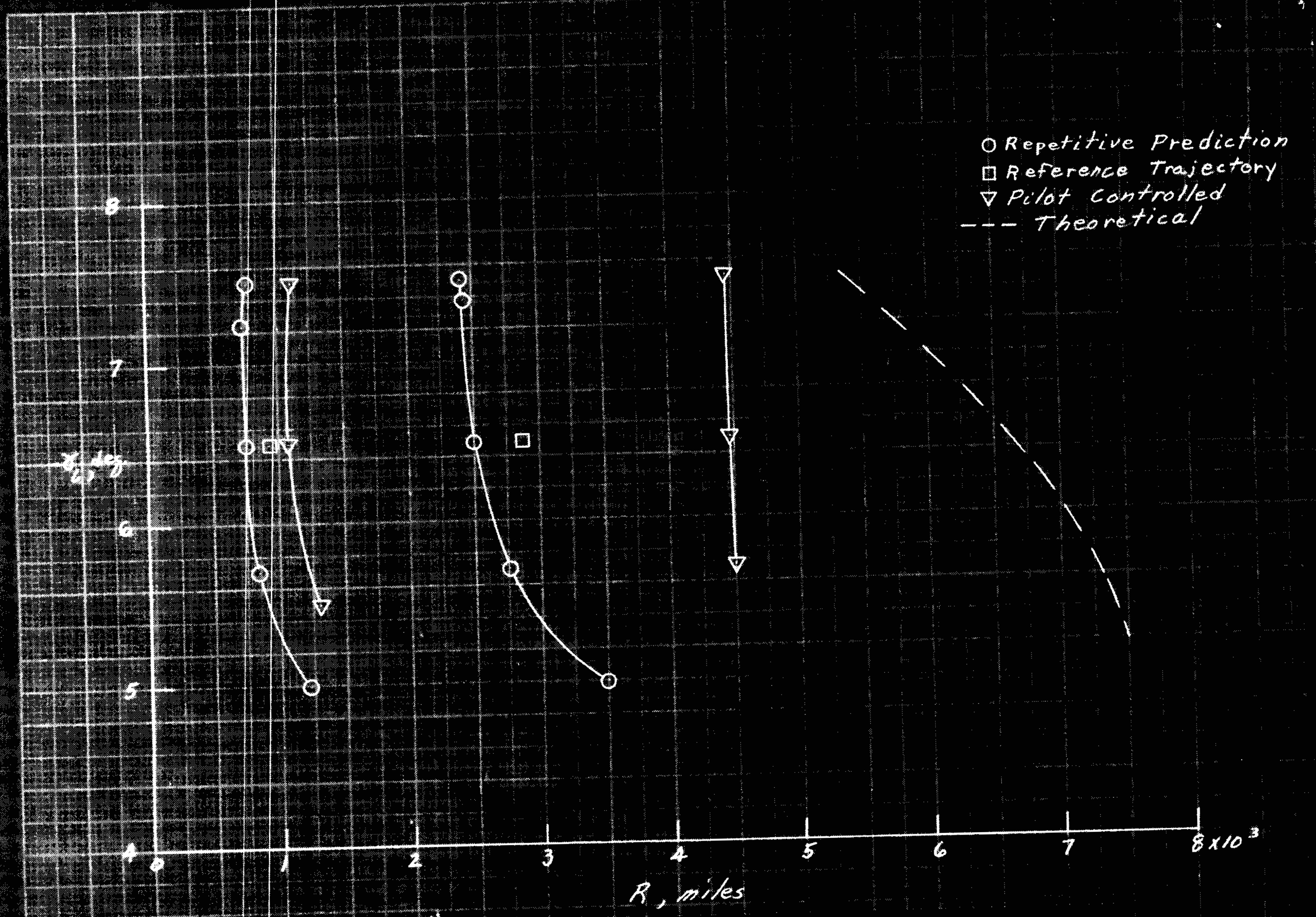

Figure 18. - Comparison of longitudinal range capability for several guidance systems.
(L/D - 1/2, V_i = 36,500 fps)

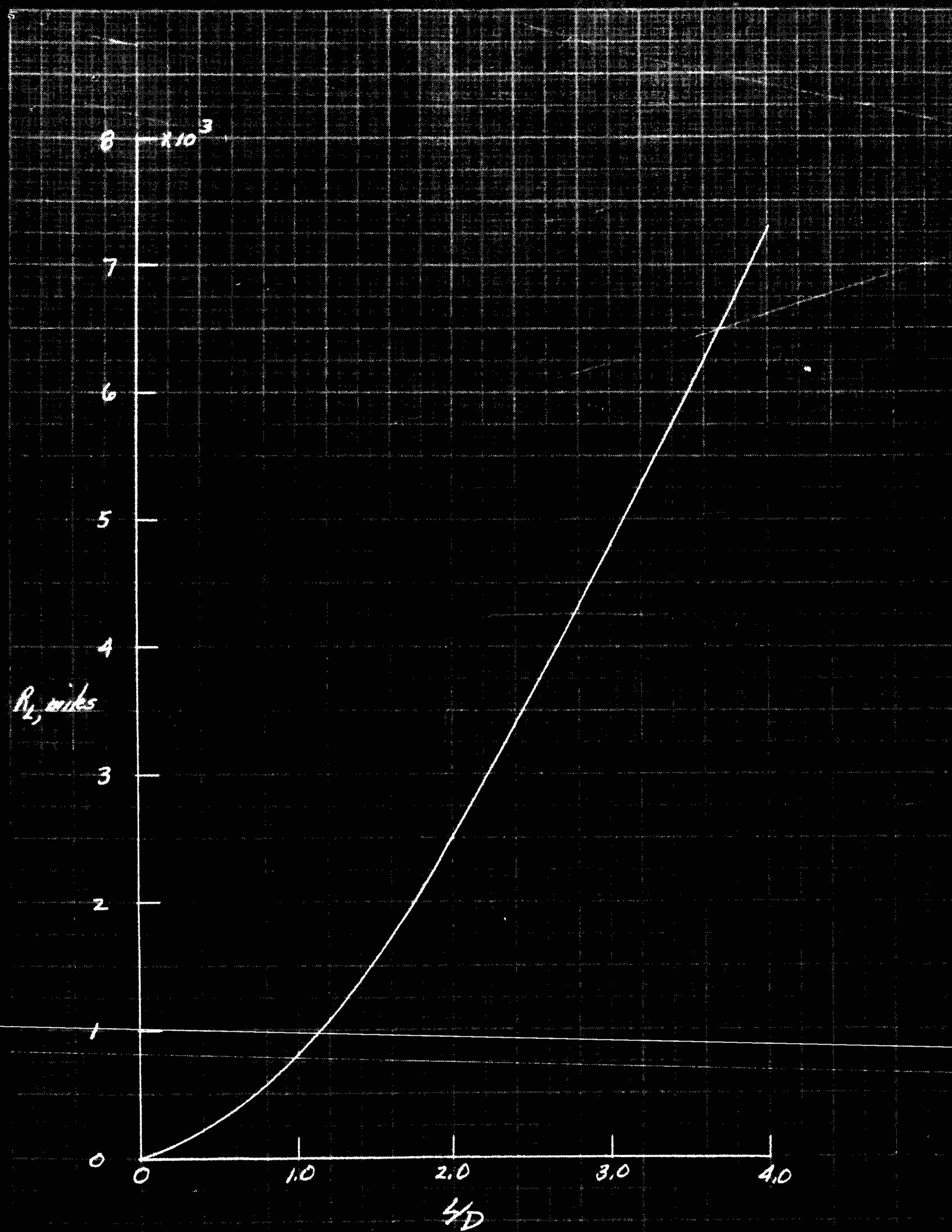

Figure 19. - Vehicle maximum lateral range capability. (V_1 = 26,000 fps)

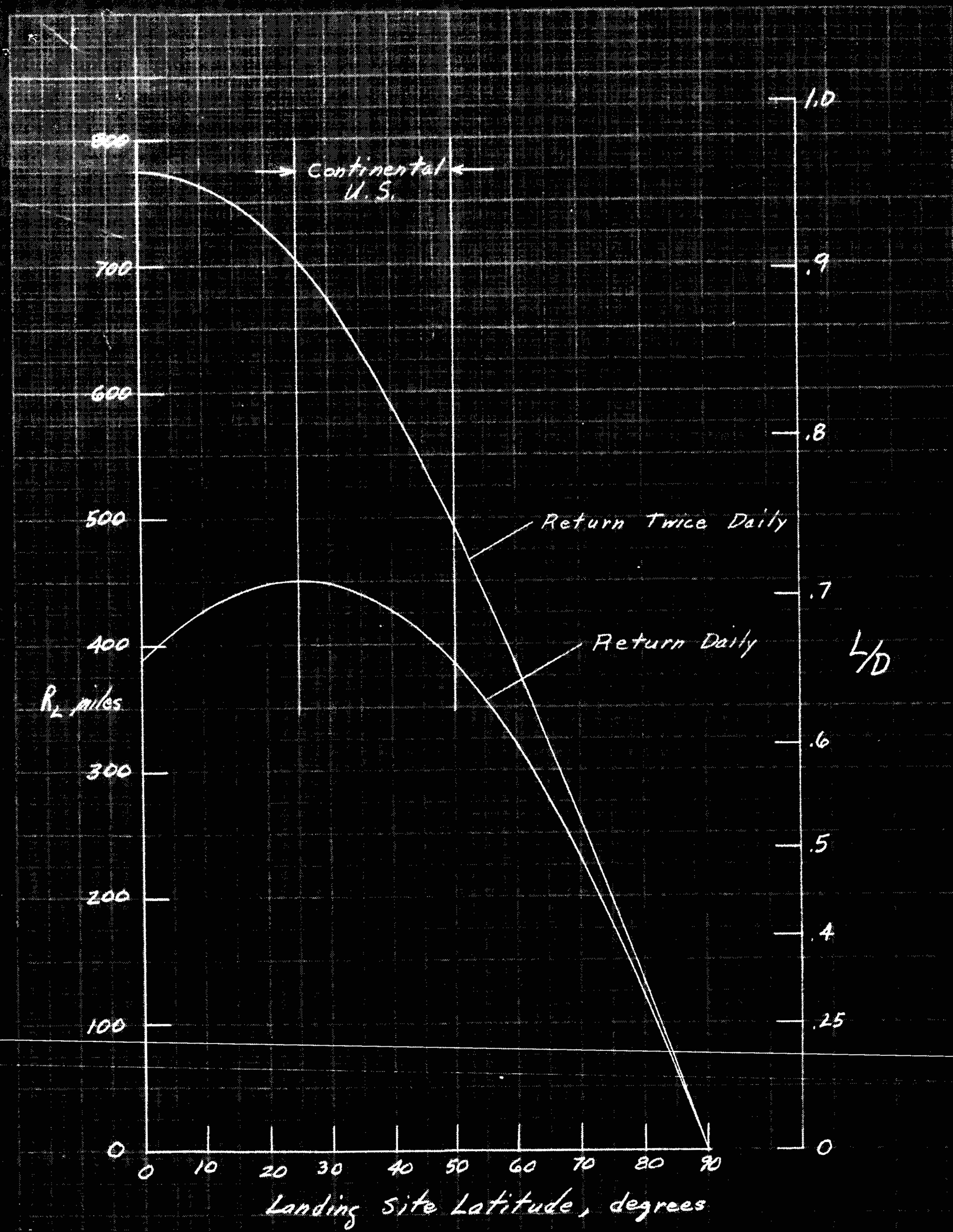

Figure 20. - Lateral range and L/D required for return from a polar orbit.
(V_i = 26,000 fps)

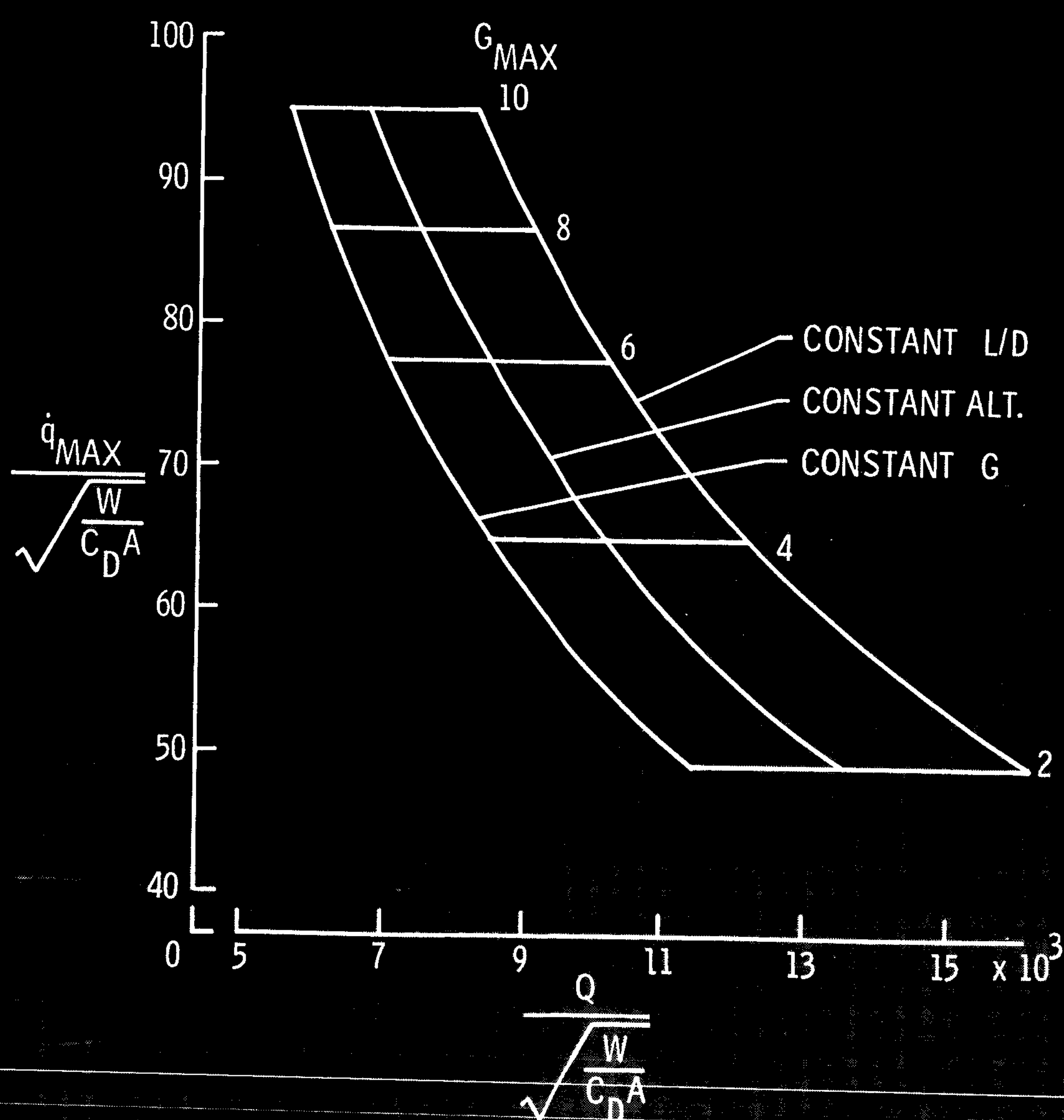

Figure 21. - Effect of reentry maneuver on convective heating.

V_i = 36,500 fps

L/D = 1/2

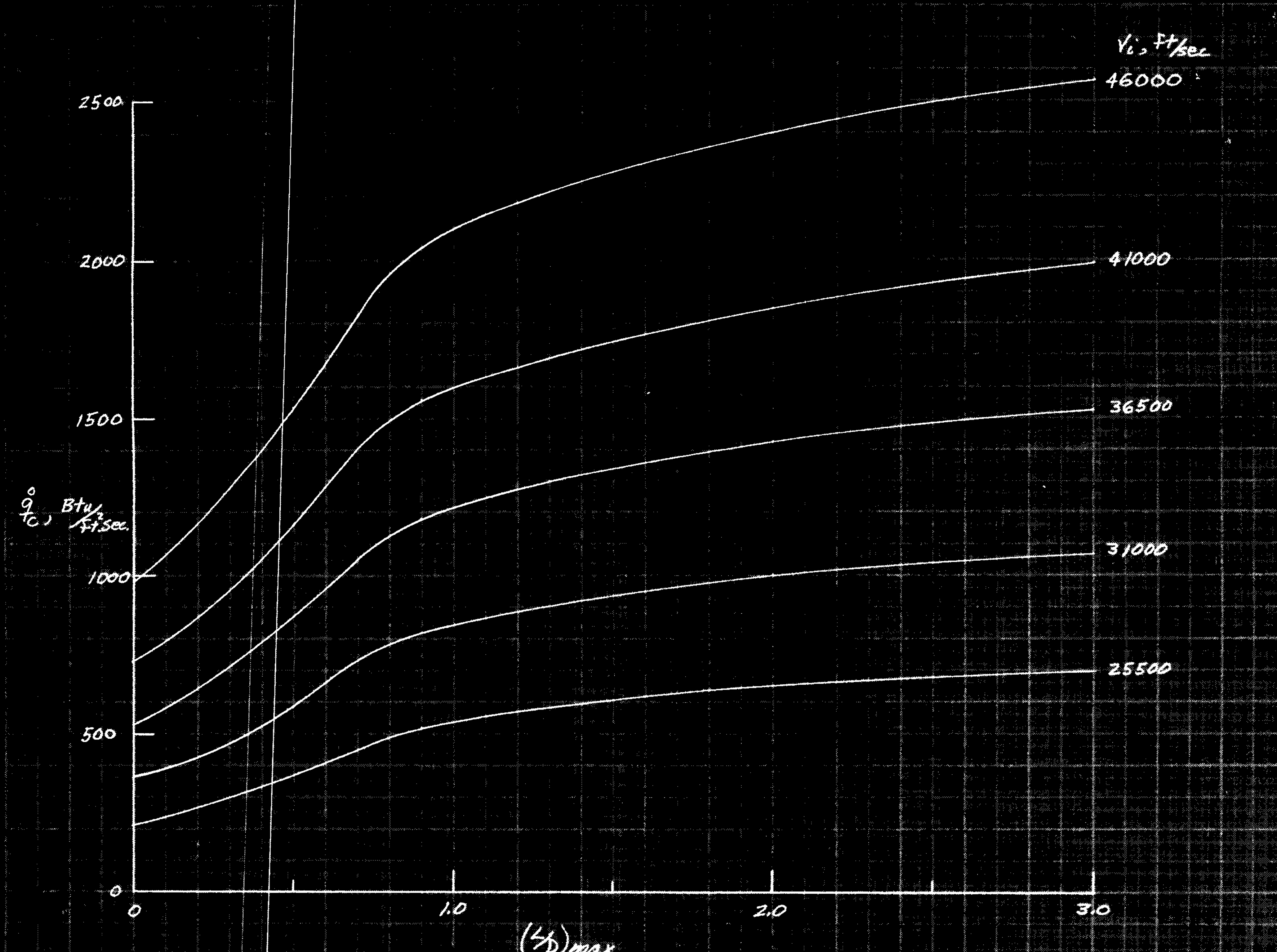

Figure 22. - Maximum convective heating rate.
(R_N = 1 ft)

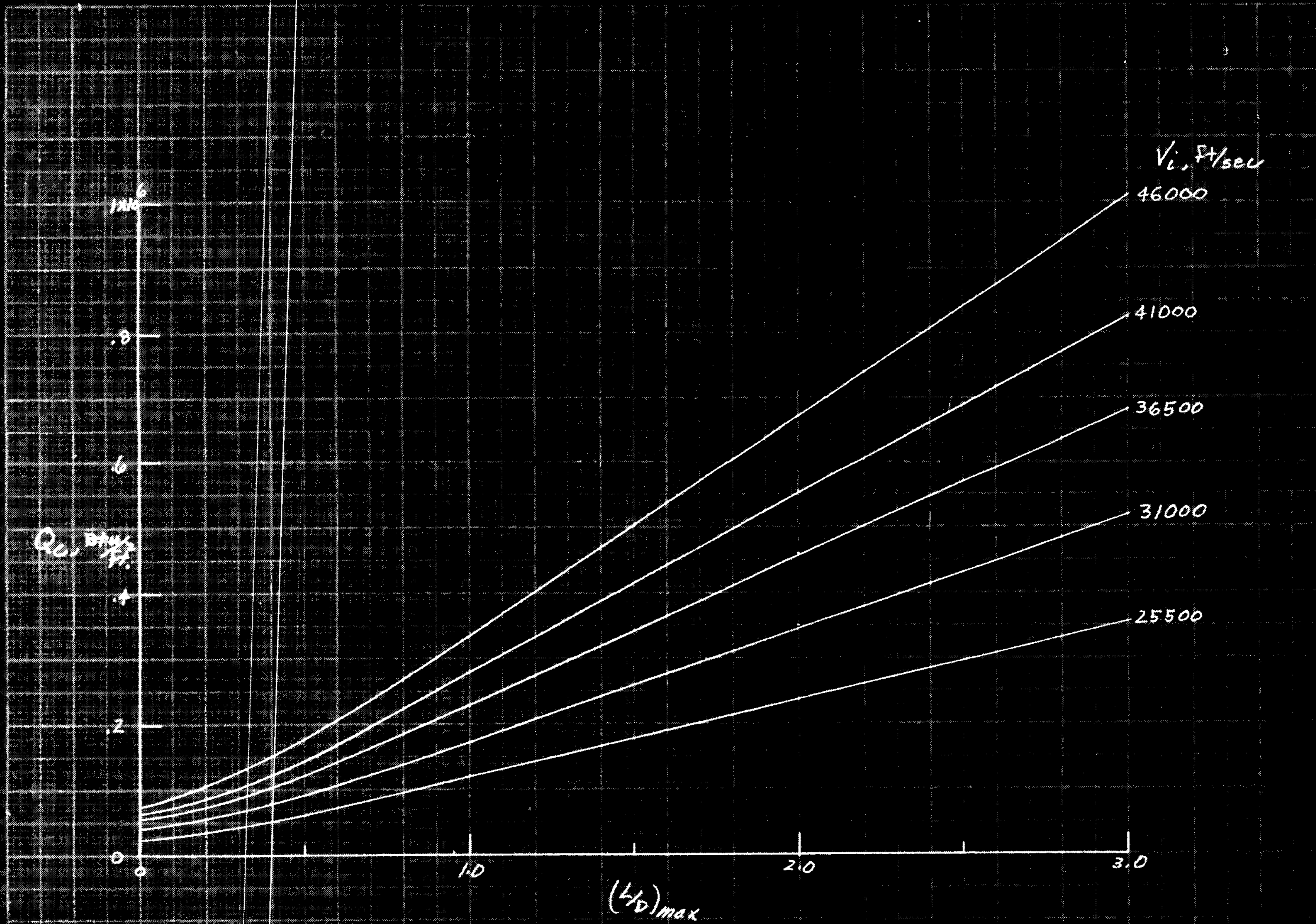

Figure 23. - Maximum convective total heat load.
(R_N = 1 ft)

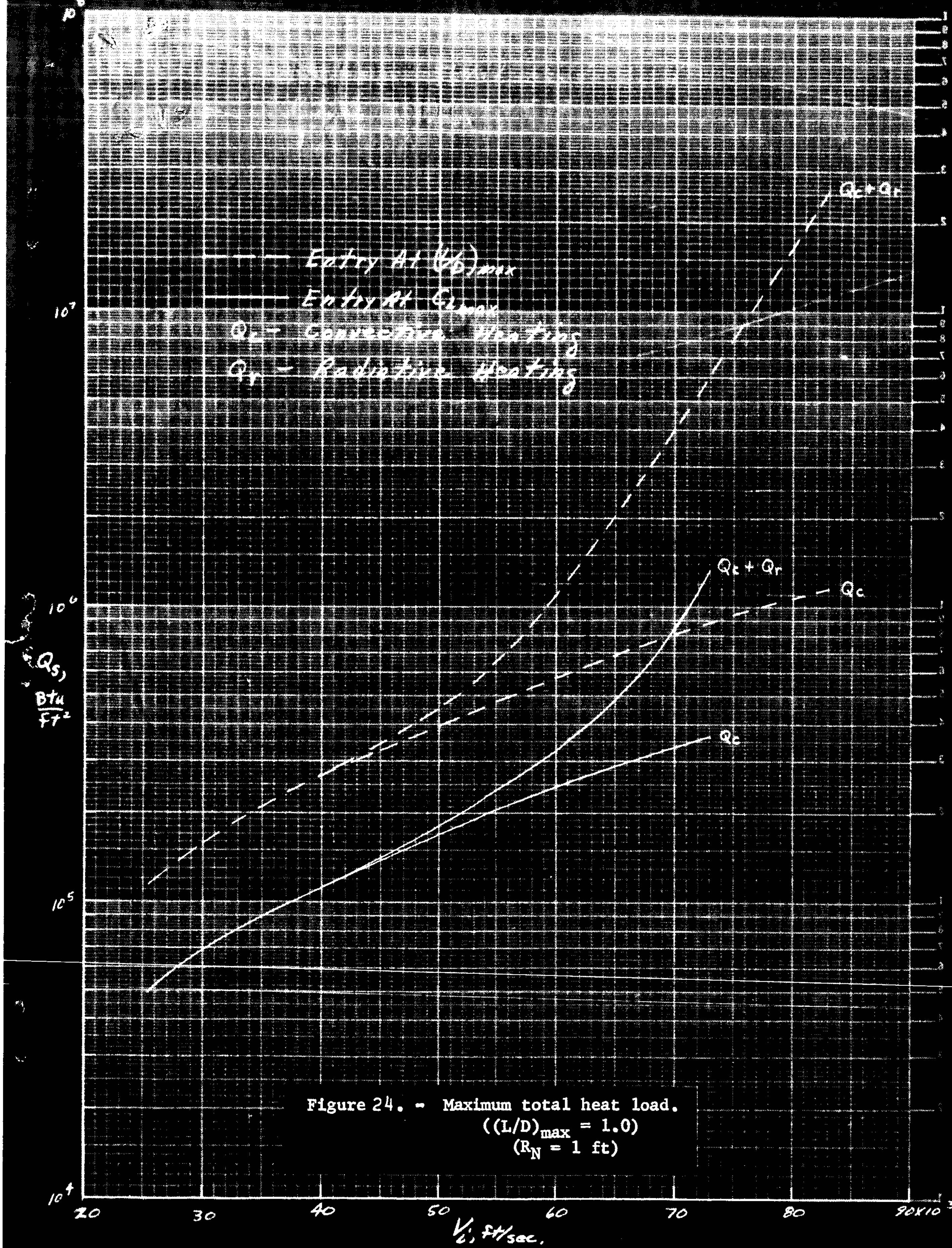

Figure 24. - Maximum total heat load.
$((L/D)_{max} = 1.0)$
$(R_N = 1\ ft)$